

# Intramolecular Ion–Ion Interactions in Zwitterionic Metallocene Olefin Polymerization Catalysts Derived from “Tucked-In” Catalyst Precursors and the Highly Electrophilic Boranes $\text{XB}(\text{C}_6\text{F}_5)_2$ ( $\text{X} = \text{H}, \text{C}_6\text{F}_5$ )

Yimin Sun,<sup>†</sup> Rupert E. v. H. Spence,<sup>‡</sup> Warren E. Piers,<sup>\*,†,1</sup> Masood Parvez,<sup>†</sup> and Glenn P. A. Yap<sup>§</sup>

Contribution from the Department of Chemistry, The University of Calgary, 2500 University Drive N.W., Calgary, Alberta T2N 1N4, Canada, NOVA Research & Technology Corp., 2928 16th Street N.E., Calgary, Alberta T2E 7K7, Canada, and Windsor Molecular Structure Center, Department of Chemistry and Biochemistry, University of Windsor, Windsor, Ontario N9B 3P4, Canada

Received January 16, 1997<sup>⊗</sup>

**Abstract:** The reactions of so called “tuck-in” permethyl zirconocene compounds  $\text{Cp}^*(\eta^5\text{-}\eta^1\text{-C}_5\text{Me}_4\text{CH}_2)\text{ZrX}$  ( $\text{X} = \text{Cl}$  (**1a**),  $\text{C}_6\text{H}_5$  (**1b**),  $\text{CH}_3$  (**1c**)) with the highly electrophilic boranes  $\text{HB}(\text{C}_6\text{F}_5)_2$  and  $\text{B}(\text{C}_6\text{F}_5)_3$  are described. The products are zwitterionic olefin polymerization catalysts. Reactions with **1a** and **1b** yielded single products cleanly, but reactions with tuck-in methyl starting material **1c** gave mixtures. Spectroscopic and structural studies showed that the electrophilic zirconium center in the product zwitterions was stabilized by a variety of mechanisms. In the products of reaction between **1a** and **1b** with  $\text{HB}(\text{C}_6\text{F}_5)_2$ ,  $\text{Cp}^*[\eta^5\text{-}\eta^1\text{-C}_5\text{Me}_4\text{CH}_2\text{B}(\text{C}_6\text{F}_5)_2(\mu\text{-H})]\text{ZrX}$  ( $\text{X} = \text{Cl}$  (**2a**), 74%),  $\text{C}_6\text{H}_5$  (**2b**, 62%)), the metal is chelated by a pendant hydridoborate moiety. Chloride product **2a** was characterized crystallographically. In the reaction of  $\text{B}(\text{C}_6\text{F}_5)_3$  with **1a**, the fluxional zwitterionic product  $\text{Cp}^*[\eta^5\text{-}\eta^1\text{-C}_5\text{Me}_4\text{CH}_2\text{B}(\text{C}_6\text{F}_5)_3]\text{ZrCl}$  (**3a**, 84%) is stabilized by a weak donor interaction between one of the *ortho* fluorine atoms of the  $-\text{CH}_2\text{B}^-(\text{C}_6\text{F}_5)_3$  counterion and the zirconium center ( $\text{Zr-F} = 2.267(5)$  Å). In the product of the reaction between **1b** and  $\text{B}(\text{C}_6\text{F}_5)_3$ ,  $\text{Cp}^*[\eta^5\text{-}\eta^1\text{-C}_5\text{Me}_4\text{CH}_2\text{B}(\text{C}_6\text{F}_5)_3]\text{ZrC}_6\text{H}_5$  (**3b**, 82%), a similar *ortho*-fluorine interaction was found in a yellow kinetic product (**y-3b**), which converted upon heating gently to a thermodynamic orange polymorph (**o-3b**) in which the zirconium center is compensated via an agostic interaction from an *ortho* C–H bond of the phenyl group and an interaction between the methylene group of the  $-\text{CH}_2\text{B}^-(\text{C}_6\text{F}_5)_3$  counteranion. These compounds were both characterized by X-ray crystallography. Zwitterion **o-3b** reacts with  $\text{H}_2$  to form the zwitterionic hydride  $\text{Cp}^*[\eta^5\text{-}\eta^1\text{-C}_5\text{Me}_4\text{CH}_2\text{B}(\text{C}_6\text{F}_5)_3]\text{ZrH}$  (**4**, 77%), characterized by NMR spectroscopy and X-ray crystallography to reveal a return to the *ortho*-fluorine mode of stabilization. Compounds **2a**, **3a**, **o-3b**, and **4** were all found to be active ethylene polymerization catalysts; the chloride derivatives required minimal amounts of methylaluminoxane (MAO) to alkylate the zirconium center. Polymerization data are discussed in light of the structural findings for the catalysts employed.

## Introduction

Polyolefins produced by group 4 metal metallocene based technologies are gaining an increasing share of the worldwide plastics market.<sup>2</sup> After a decade of intense research activity in both industrial and academic laboratories, the details of the means by which these catalysts mediate the polymerization reaction are now relatively well understood.<sup>3</sup> Fourteen-electron cationic species<sup>4</sup> are commonly presumed to be responsible for olefin enchainment while activity<sup>5</sup> and stereoregularity<sup>6,3b</sup> are modulated by the steric/electronic properties of the ancillary

ligand set and the ion–ion interactions present between this highly electrophilic cation and its counteranion.<sup>7</sup> Although the affect of ion pairing on activity is not intimately understood, generally strong ion–ion interactions lead to lower polymerization activity as the counterion blocks the olefin monomer from the active site of the catalyst. Consequently, the nature of the cocatalyst or activator employed to generate the active cations responsible for catalysis often has a significant effect on the behavior of the resultant catalyst system.<sup>8</sup> The two most important classes of catalyst activators are methylaluminoxane

<sup>†</sup> The University of Calgary.

<sup>‡</sup> NOVA Research & Technology Corp.

<sup>§</sup> University of Windsor.

<sup>⊗</sup> Abstract published in *Advance ACS Abstracts*, May 1, 1997.

(1) Author to whom correspondence may be addressed. FAX: 403-289-9488. E-mail: wpiers@chem.ucalgary.ca.

(2) Thayer, A. M. *Chem. Eng. News* **1995**, 73 (37), 15.

(3) (a) Mohring, P. C.; Coville, N. J. *J. Organomet. Chem.* **1994**, 479, 1. (b) Brintzinger, H. H.; Fischer, D.; Mulhaupt, R.; Rieger, B.; Waymouth, R. M. *Angew. Chem., Int. Ed. Engl.* **1995**, 34, 1143. (c) Bochmann, M. *J. Chem. Soc., Dalton Trans.* **1996**, 255. (d) Marks, T. J. *Acc. Chem. Res.* **1992**, 25, 57.

(4) (a) Jordan, R. F. *Adv. Organomet. Chem.* **1991**, 32, 325. (b) Jordan, R. F.; Bradley, P. K.; LaPointe, R. E.; Taylor, D. F. *New J. Chem.* **1990**, 14, 505.

(5) (a) Piccolrovazzi, N.; Pino, P.; Consiglio, G.; Sironi, A.; Moert, M. *Organometallics* **1990**, 9, 3098. (b) Lee, I. K.; Gauthier, W. J.; Ball, J. M.; Iyengary, B.; Collins, S. *Organometallics* **1992**, 11, 2115. (c) Collins, S.; Gauthier, W. J.; Holden, D. A.; Kuntz, B. A.; Taylor, N. J.; Ward, D. G. *Organometallics* **1991**, 10, 2061.

(6) (a) Herzog, T. A.; Zubris, D. L.; Bercaw, J. E. *J. Am. Chem. Soc.* **1996**, 118, 11988. (b) Gilchrist, J. H.; Bercaw, J. E. *J. Am. Chem. Soc.* **1996**, 118, 12021.

(7) (a) Richardson, D. E.; Alameddin, N. G.; Ryan, M. F.; Hayes, T.; Eyler, J. R.; Siedle, A. R. *J. Am. Chem. Soc.* **1996**, 118, 11244. (b) Deck, P. A.; Marks, T. J. *J. Am. Chem. Soc.* **1995**, 117, 6128. (c) Siedle, A. R.; Newmark, R. A. *J. Organomet. Chem.* **1995**, 497, 119. (d) Vizzini, J. C.; Chien, J. C. W.; Gaddam, N. B.; Newmark, R. A. *J. Polym. Sci. A, Polym. Chem.* **1994**, 32, 2049. (e) Giardello, M. A.; Eisen, M. S.; Stern, C. L.; Marks, T. J. *J. Am. Chem. Soc.* **1993**, 115, 3326. (f) Jia, L.; Yang, X.; Ishihara, A.; Marks, T. J. *Organometallics* **1995**, 14, 3135.

(MAO)<sup>9</sup> based and those yielding polyfluorinated borate counterions (e.g., B(C<sub>6</sub>F<sub>5</sub>)<sub>3</sub>,<sup>10</sup> [HNR<sub>3</sub>]<sup>+</sup>[B(C<sub>6</sub>F<sub>5</sub>)<sub>4</sub>]<sup>-</sup>,<sup>11</sup> or [Ph<sub>3</sub>C]<sup>+</sup>[B(C<sub>6</sub>F<sub>5</sub>)<sub>4</sub>]<sup>-</sup>). Given the impact ion–ion interactions can have on polymerization activity, a detailed understanding of these contacts is necessary for the rational design of new catalysts and/or new activators.<sup>13</sup>

While little is known regarding [Cp<sub>2</sub>MR]<sup>+</sup>[MAO]<sup>-</sup> interactions,<sup>14</sup> several classes of [Cp<sub>2</sub>MR]<sup>+</sup>[borate]<sup>-</sup> contacts have been structurally and/or spectroscopically established. For example, when cationic metallocenes with borate counterions of the general formula [XB(C<sub>6</sub>F<sub>5</sub>)<sub>3</sub>]<sup>-</sup> (X = C<sub>6</sub>F<sub>5</sub>, H, or an abstracted alkyl group) are generated in the absence of Lewis base donors, the borate counterion may stabilize the highly Lewis acidic metal center via a fluorine atom lone pair,<sup>15</sup> a three-center two-electron μ-hydride<sup>16</sup> or methyl bridge,<sup>17</sup> or the arene π-system of an abstracted benzyl group.<sup>18</sup>

One strategy for controlling ion–ion interactions is to prepare zwitterionic catalysts wherein the charges are physically separated by covalent attachment of a borate counterion within the ancillary structure of the supporting ligand of the catalyst. Hlatky and Turner<sup>19</sup> had early success using this tactic, producing highly active zwitterionic catalysts incorporating borate- and carborane-type counterions. More recently the groups of Bochmann<sup>20</sup> and Erker<sup>21</sup> have taken diverse synthetic approaches toward zwitterionic catalysts. Although these compounds exhibit ethylene polymerization activities akin to non-zwitterionic analogs, quantitative comparison studies to show that higher activities can be achieved by enforced charge separation are yet to be done.

Our initial attempts to prepare zwitterionic catalysts for olefin polymerization involved hydroboration of olefinic groups attached to the cyclopentadienyl ligand framework of conventional metallocene catalysts<sup>22</sup> with use of the highly electrophilic borane reagent [HB(C<sub>6</sub>F<sub>5</sub>)<sub>2</sub>]<sub>2</sub>.<sup>23</sup> During the course of these studies, we found that HB(C<sub>6</sub>F<sub>5</sub>)<sub>2</sub>, in addition to hydroborating the pendant olefin, reacted with the Zr–C bonds of alkyl compounds containing these ligands. Separate studies revealed

(8) For example, the contrasting results found in the following references may be attributed to counterion effects. a) Scollard, J. D.; McConville, D. H. *J. Am. Chem. Soc.* **1996**, *118*, 10008. b) Scollard, J. D.; McConville, D. H.; Payne, N. C.; Vittal, J. J. *Macromolecules* **1996**, *29*, 5241.

(9) Sinn, H.; Kaminsky, W. *Adv. Organomet. Chem.* **1980**, *18*, 99.

(10) (a) Massey, A. G.; Park, A. J. *J. Organomet. Chem.* **1964**, *2*, 245.

(b) Yang, X.; Stern, C. L.; Marks, T. J. *J. Am. Chem. Soc.* **1991**, *113*, 3623.

(11) Yang, X.; Stern, C. L.; Marks, T. J. *Organometallics* **1991**, *10*, 840.

(12) (a) Bochmann, M.; Lancaster, S. J. *J. Organomet. Chem.* **1992**, *434*, C1.

(b) Chien, J. C. W.; Tsai, W. M.; Rausch, M. D. *J. Am. Chem. Soc.* **1991**, *113*, 8570.

(13) Chen, Y.-X.; Stern, C. L.; Yang, S.; Marks, T. J. *J. Am. Chem. Soc.* **1996**, *118*, 12451.

(14) Harlan, C. J.; Bott, S. G.; Barron, A. R. *J. Am. Chem. Soc.* **1995**, *117*, 6465.

(15) Horton, A. D.; Orpen, A. G. *Organometallics* **1991**, *10*, 3910.

(16) (a) Spence, R. E. v. H.; Parks, D. J.; Piers, W. E.; MacDonald, M.; Zaworotko, M. J.; Rettig, S. J. *Angew. Chem., Int. Ed. Engl.* **1995**, *34*, 1230.

(b) Sun, Y.; Piers, W. E.; Rettig, S. J. *Organometallics* **1996**, *15*, 4110.

(17) Yang, X.; Stern, C. L.; Marks, T. J. *J. Am. Chem. Soc.* **1994**, *116*, 10015.

(18) (a) Bochmann, M.; Lancaster, S. J.; Hursthouse, M. B.; Abdul Malik, K. M. *Organometallics* **1994**, *13*, 2235. (b) Bochmann, M.; Lancaster, S. J. *Makromol. Chem. Rapid Commun.* **1993**, *14*, 807. (c) Bochmann, M.; Lancaster, S. J. *Organometallics* **1993**, *12*, 633. (d) Pellecchia, C.; Immirzi, A.; Grassi, A.; Zambelli, A. *Organometallics* **1994**, *13*, 4473.

(19) Hlatky, G. G.; Turner, H. W.; Eckman, R. R. *J. Am. Chem. Soc.* **1989**, *111*, 2728.

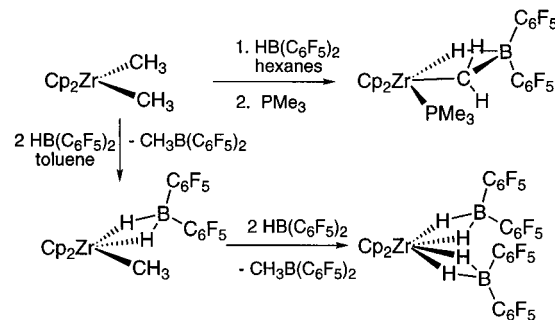
(20) Bochmann, M.; Lancaster, S. J.; Robinson, O. B. *J. Chem. Soc., Chem. Commun.* **1995**, 2081.

(21) (a) Ruwwe, J.; Erker, G.; Fröhlich, R. *Angew. Chem., Int. Ed. Engl.* **1996**, *35*, 80. (b) Temme, B.; Karl, J.; Erker, G. *Chem. Eur. J.* **1996**, *2*, 919. (c) Temme, B.; Erker, G.; Karl, J.; Luftmann, H.; Fröhlich, R.; Kotila, S. *Angew. Chem., Int. Ed. Engl.* **1995**, *34*, 1755.

(22) Spence, R. E. v. H.; Piers, W. E. *Organometallics* **1995**, *14*, 4617.

(23) (a) Parks, D. J.; Spence, R. E. v. H.; Piers, W. E. *Angew. Chem., Int. Ed. Engl.* **1995**, *34*, 809. (b) Piers, W. E.; Spence, R. E. v. H. U.S. Patent 5,496,960, March 5, 1996 (University of Guelph).

### Scheme 1. Reactions of Cp<sub>2</sub>Zr(CH<sub>3</sub>)<sub>2</sub> with HB(C<sub>6</sub>F<sub>5</sub>)<sub>2</sub>



two competing pathways by which HB(C<sub>6</sub>F<sub>5</sub>)<sub>2</sub> reacts with simple zirconocene *bis*-alkyls (Scheme 1).<sup>16a</sup> One involved loss of alkane to produce borane-stabilized alkylidene derivatives of zirconocene, while the other was an alkyl/hydride exchange reaction<sup>24</sup> followed by complexation of HB(C<sub>6</sub>F<sub>5</sub>)<sub>2</sub> to the newly formed Zr–H moiety, giving borate derivatives. While interesting, this chemistry ran counter to the goal of forming zwitterionic compounds capable of polymerizing olefins in the absence of further cocatalysts.

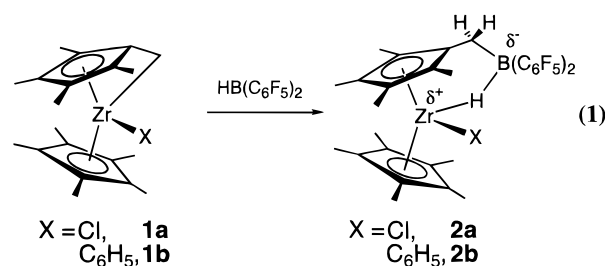
We decided to utilize the alkyl/hydride exchange reaction to our advantage and treat group 4 metallocene compounds with tethered alkyl ligands with HB(C<sub>6</sub>F<sub>5</sub>)<sub>2</sub> to prepare zwitterionic compounds. One family of compounds with the requisite tethered alkyl functionality are the so-called “tucked-in” permethyl metallocenes in which one of the C<sub>5</sub>Me<sub>5</sub> (Cp\*) methyl groups has undergone metallation and is σ bound to the metal center. Several such compounds are known, including the tuck-in chloro, phenyl, and methyl derivatives Cp\*(C<sub>5</sub>Me<sub>4</sub>CH<sub>2</sub>)ZrX (X = Cl (**1a**),<sup>25</sup> C<sub>6</sub>H<sub>5</sub> (**1b**),<sup>26</sup> CH<sub>3</sub> (**1c**)). Herein we describe the reactions of these tuck-in precursors with both HB(C<sub>6</sub>F<sub>5</sub>)<sub>2</sub> and the more common activator B(C<sub>6</sub>F<sub>5</sub>)<sub>3</sub>. The zwitterionic products provide structural insights into cation–anion interactions and are highly active olefin polymerization catalysts which do not require other cocatalysts.

## Results and Discussion

### Reactions of Tucked-In Zirconocenes with HB(C<sub>6</sub>F<sub>5</sub>)<sub>2</sub>

Tuck-in precursors **1a** and **1b** were prepared according to literature procedures<sup>25,26</sup> by thermal elimination of RH from Cp\*<sub>2</sub>Zr(Cl)CH<sub>2</sub>CMe<sub>3</sub> and Cp\*<sub>2</sub>Zr(C<sub>6</sub>H<sub>5</sub>)<sub>2</sub>, respectively. The tuck-in methyl compound **1c** was prepared straightforwardly from chloro complex **1a** and MeLi and isolated as a red powder in 83% yield.

The chloro and phenyl tuck-in compounds reacted rapidly and cleanly with 1 equiv of HB(C<sub>6</sub>F<sub>5</sub>)<sub>2</sub> and 100% regioselectivity for the metallated Zr–C bond (eq 1), yielding zwitterionic



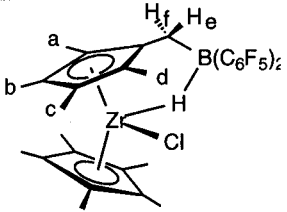
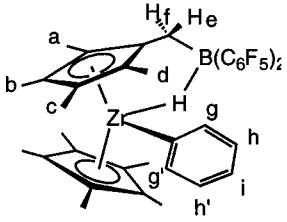
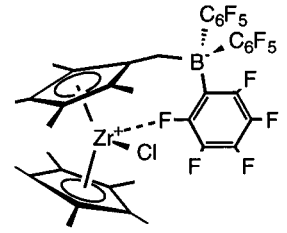
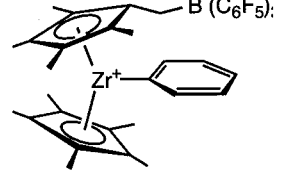
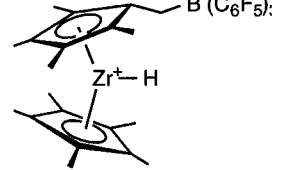
complexes **2a** and **2b** in excellent yield. (All new compounds were characterized by <sup>1</sup>H, <sup>13</sup>C, <sup>19</sup>F, and <sup>11</sup>B NMR spectroscopy; these data are collected in Tables 1 and 2.) For compounds **2**,

(24) Marsella, J. A.; Caulton, K. G. *J. Am. Chem. Soc.* **1982**, *104*, 2361.

(25) Tjaden, E. B.; Stryker, J. M. *J. Am. Chem. Soc.* **1993**, *115*, 2083.

(26) Schock, L. E.; Brock, C. P.; Marks, T. J. *Organometallics* **1987**, *6*, 232.

**Table 1.**  $^1\text{H}$  and  $^{13}\text{C}\{^1\text{H}\}$  NMR Data for Isolated New Compounds<sup>a</sup>

Compound	#	$^1\text{H}$ NMR Data			$^{13}\text{C}\{^1\text{H}\}$ NMR Data <sup>b</sup>	
		$\delta(\text{ppm})$	Assign.	J(Hz)	$\delta(\text{ppm})$	Assign.
	<b>2a</b>	3.11 (d, 1H)	Hf	14.4	126.3	$\text{C}_5(\text{CH}_3)_5$
		2.88 (d, d, 1H)	He	4.9	14.8 (br)	$\text{BCH}_2$
		1.79, 1.47 (s, 6H)	$\text{CH}_3$ a, d		11.2	$\text{C}_5(\text{CH}_3)_5$
		1.74, 1.51 (s, 6H)	$\text{CH}_3$ c, b		12.6, 11.9	$\text{C}_5(\text{CH}_3)_4$
		1.63 (s, 15H)	$\text{C}_5(\text{CH}_3)_5$		11.1, 10.5	$\text{C}_5(\text{CH}_3)_4$
		0.5 (br, 1H)	$\mu\text{-ZrHB}$			
	<b>2b</b>	7.47, 7.02 (m, 2H)	h, h'	7.2, 7.2	124.0, 123.2, 120.9,	$\text{C}_5(\text{CH}_3)_4$
		7.19 (m, 1H)	i		112.2	
		7.41, 6.05 (d, 2H)	g', g	7.1, 7.0	122.1	$\text{C}_5(\text{CH}_3)_5$
		3.64, 2.43 (d, 2H)	Hf, He	14.9	134.5, 104.2	<i>o</i> - $\text{C}_6\text{H}_5$ g', g
		2.03, 0.67 (s, 6H)	$\text{CH}_3$ a, d		130.4, 127.9	<i>m</i> - $\text{C}_6\text{H}_5$ h', h
		1.51, 1.43 (s, 6H)	$\text{CH}_3$ c, b		127.6	<i>p</i> - $\text{C}_6\text{H}_5$
		1.40 (s, 15H)	$\text{C}_5(\text{CH}_3)_5$		15.3 (br)	$\text{BCH}_2$
		0.35 (br, 1H)	$\mu\text{-ZrHB}$		11.4, 10.5	$\text{C}_5(\text{CH}_3)_4$ a, d
					12.6, 11.2	$\text{C}_5(\text{CH}_3)_4$ c, b
					11.0	$\text{C}_5(\text{CH}_3)_5$
	<b>3a</b>	2.98 (br, 2H)	$\text{CH}_2\text{B}$		127.5	$\text{C}_5(\text{CH}_3)_5$
		1.75 (s)	$\text{C}_5(\text{CH}_3)_5$		11.3 (br)	$\text{C}_5(\text{CH}_3)_5$
		1.42 (br s, 15H)	$\text{C}_5(\text{CH}_3)_5$		27.0 (br)	$\text{BCH}_2$
		1.65, 1.35 (br s, 6H, 6H)	$\text{C}_5(\text{CH}_3)_4$		12.7 (br)	$\text{C}_5(\text{CH}_3)_4$
		3.43, 2.77	$\text{CH}_2\text{B}$			
		1.28, 1.51, 1.65, 1.90	$\text{C}_5(\text{CH}_3)_4$			
1.34	$\text{C}_5(\text{CH}_3)_5$					
	<b>o-3b</b>	7.17 (m, 2H)	<i>m</i> - $\text{C}_6\text{H}_5$	7.3	129.3, 125.6, 125.4	$\text{C}_5(\text{CH}_3)_{4/5}$
		7.00 (t, 1H)	<i>p</i> - $\text{C}_6\text{H}_5$		125.2	<i>o</i> - $\text{C}_6\text{H}_5$
		6.38 (d, 2H)	<i>o</i> - $\text{C}_6\text{H}_5$	7.3	126.5	<i>m</i> - $\text{C}_6\text{H}_5$
		2.45 (br s, 2H)	$\text{CH}_2\text{B}$		127.8	<i>p</i> - $\text{C}_6\text{H}_5$
		1.48, 1.02 (s, 12H)	$\text{C}_5(\text{CH}_3)_4$		23.4	$\text{BCH}_2$
		1.42 (s, 15H)	$\text{C}_5(\text{CH}_3)_5$		12.5, 11.6	$\text{C}_5(\text{CH}_3)_4$
11.2				$\text{C}_5(\text{CH}_3)_5$		
	<b>4<sup>d</sup></b>	2.85 (br, 2H)	$\text{CH}_2\text{B}$			
		1.52, 1.34 (br, 6H, 6H)	$\text{C}_5(\text{CH}_3)_4$			
		1.47 (s, 15H)	$\text{C}_5(\text{CH}_3)_5$			
		2.48 <sup>c</sup> K <sup>c</sup>				
		3.13, 2.66	$\text{CH}_2\text{B}$	13.8		
		1.73, 1.39, 1.24, 1.17	$\text{C}_5(\text{CH}_3)_4$			
1.44	$\text{C}_5(\text{CH}_3)_5$					

<sup>a</sup> All spectra were recorded in  $\text{C}_6\text{D}_6$  at room temperature unless otherwise indicated. <sup>b</sup> Unless indicated, carbons without protons attached to them were generally not observed. <sup>c</sup> Low-temperature spectra recorded in  $\text{C}_7\text{D}_8$ . <sup>d</sup> Sample not stable in solution long enough to accumulate a quality  $^{13}\text{C}$  NMR spectrum.

the diastereotopic relationship between protons and carbons with the same connectivity of the metallated Cp\* ring is retained, indicating the presence of a strong interaction between the hydridoborate counterion and the zirconium center as depicted. The  $^{19}\text{F}$  NMR spectra for both compounds **2** show that the  $\text{C}_6\text{F}_5$  groups are diastereotopic as well. The chemical shifts for the  $^{11}\text{B}$  nuclei of  $-25.4$  and  $-24.9$  ppm are diagnostic for the tetracoordinate, anionic environment of borates.<sup>27</sup> Broad resonances at about 0.4 ppm for the  $\mu\text{-H}$  protons are at a comparable chemical shift to that observed for those of the dihydridoborate complex  $\text{Cp}_2\text{Zr}[(\mu\text{-H})_2\text{B}(\text{C}_6\text{F}_5)_2]_2$  (0.38 ppm).<sup>16a</sup> The resonances due to the Cp\* ligand for **2a** and **2b** are shifted upfield by about 0.2–0.4 ppm relative to tuck-in compounds **1**; this shift is common to all of the new compounds described herein and signals that boration of the metallated methylene has occurred.

In phenyl complex **2b**, resonances for the protons and carbons of the phenyl group are chemically inequivalent, suggesting restricted rotation about the  $\text{Zr}\text{-C}_{\text{ipso}}$  bond, a notion supported by the broadening and coalescence of related signals in the  $^1\text{H}$  spectrum at elevated temperatures. One of the *ortho* CH groups

in the phenyl substituent resonates at higher field than normal (*C-H*, 6.04 ppm; *C-H*, 104.2 ppm). A NOESY experiment allowed for precise assignment of all the resonances in the  $^1\text{H}$  NMR spectrum (Table 1). Based on a crosspeak between the *ortho* proton at 6.04 ppm and the broad peak at 0.4 ppm for the  $\mu\text{-H}$  of the hydridoborate moiety, the upfield *ortho* CH group must occupy the *endo* position of the metallocene wedge. The high-field chemical shift does not appear to be due to an agostic interaction between this *ortho* CH and zirconium as no supporting evidence for such an interaction was found in the IR or the NMR spectra of **2b**. A similar upfield shift in the tuck-in phenyl derivative **1b** was rationalized on the basis of hindered rotation of the ligand fixing one of the *ortho* C–H groups in an unusual magnetic environment.<sup>26</sup>

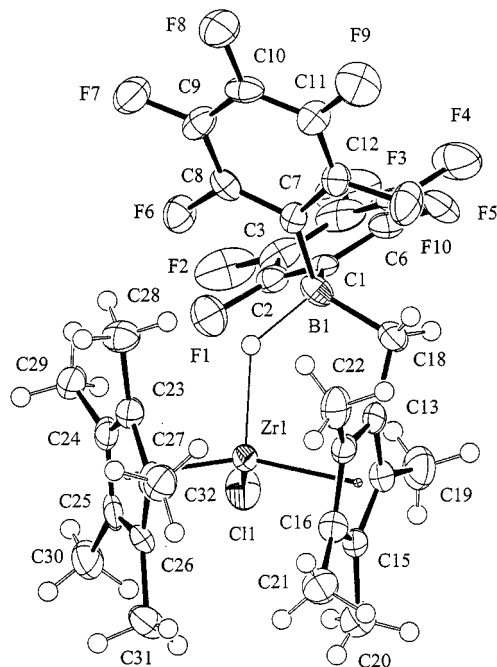
A strong chelating borate interaction between  $\text{-B-H}^-$  and the zirconium center was confirmed in an X-ray structural analysis of **2a**. An ORTEP diagram of the molecule is shown in Figure 1. Selected bond lengths for crystallographically characterized molecules in this paper are given in Table 3; pertinent angles are found in Table 4. For **2a**, the hydrogen atom bridging boron and zirconium was located on the difference Fourier map and fixed at this position. The  $\text{Zr-H}$  distance

(27) Kidd, R. G. In *NMR of Newly Accessible Nuclei*, Volume 2; Laszlo, P., Ed.; Academic Press: New York, 1983; Vol. 2.

**Table 2.**  $^{19}\text{F}$  and  $^{11}\text{B}$  NMR Data for New Compounds<sup>a</sup>

	$^{19}\text{F}$ NMR <sup>b</sup>			$^{11}\text{B}$ NMR
	<i>o</i> -F	<i>m</i> -F	<i>p</i> -F	
<b>2a</b>	-130.5 -131.1	-163.7	-157.6 -158.4	-25.4
<b>2b</b>	-129.1 -130.4	-164.1	-158.5 -159.2	-24.9
<b>3a</b>	-140.9	-162.0	-159.1	-13.8
<b>3a<sup>c</sup></b>	-128.6 -128.7(2) -130.6 -134.1 -167.7	-159.1 -159.5 -163.2 -163.5 -163.8 -164.4	-155.9(2) -156.4	
<b>o-3b</b>	-134.1	-165.7	-159.4	-13.3
<b>o-3b<sup>d</sup></b>	-127.1 -131.8 -148.0(br)	-160.7 -163.7 -164.4	-157.1(2) -159.7	
<b>4</b>	-133.1	-162.6	-159.2	-13.4
<b>4<sup>e</sup></b>	-127.2 -129.3 -130.1 -134.1 -143.3(br)	-155.7 -156.5 -163.0 -163.5 -164.5	-158.9 -159.5 -161.1	

<sup>a</sup> All values are chemical shifts in  $\text{C}_6\text{D}_6$ .  $^{19}\text{F}$  spectra were referenced to  $\text{C}_6\text{F}_6$  at  $-163.0$  ppm;  $^{11}\text{B}$  spectra were referenced to  $\text{BF}_3\cdot\text{Et}_2\text{O}$  at  $0.0$  ppm. <sup>b</sup> Many of the fluorine signals were broadened at room temperature. <sup>c</sup>  $-61$  °C. <sup>d</sup>  $-72$  °C. <sup>e</sup>  $-85$  °C.

**Figure 1.** ORTEP drawing of **2a**.

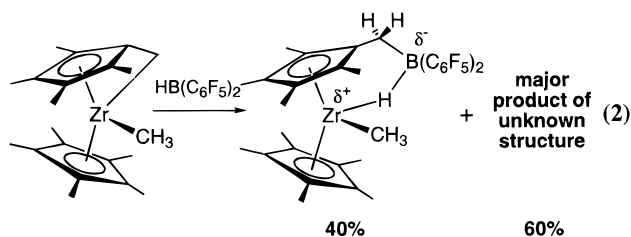
is typical for such bonds as compared with related hydridoborate compounds,<sup>28</sup> but the B–H distance of  $1.53$  Å is somewhat elongated due to the constraints of the chelate structure. The chelating borate linkage is positioned such that the bridging hydride occupies one of the coordination sites available in the plane bisecting the Cp donors; the Cl–Zr–H angle is  $99.6^\circ$ . Metrical parameters for the Cp\* ring to which the borate counterion is attached are for the most part undistorted compared with the unsubstituted Cp\* ring in the molecule. Worthy of particular note, however, is the fact that C(18) is tilted away from zirconium out of the plane defined by the five cyclopentadienyl carbons by only  $2^\circ$ , compared to tilt angles of  $\approx 4$ – $6^\circ$  for the rest of the ring methyl groups in the molecule. Thus,

(28) For example, Zr–H<sub>avg</sub> and B–H<sub>avg</sub> in the compound  $\text{Cp}_2\text{Zr}[(\mu\text{-H})_2\text{B}(\text{C}_6\text{F}_5)_2]_2$  are  $2.07$  and  $1.24$  Å, respectively. Sun, Y.; Piers, W. E.; Parvez, M. Unpublished results.

the  $\text{HB}(\text{C}_6\text{F}_5)_2$  reagent is able to add to the Zr–C bonds in **1a–b** to form borate-stabilized zwitterions relatively free of internal strain.

Stabilization of electrophilic metal centers by B–H bonds has precedent in related compounds from our lab,<sup>16</sup> in cationic zirconocenes containing carborane counterions,<sup>19,29</sup> and in neutral scandium derivatives incorporating dicarbollide ancillary ligands.<sup>30</sup> In some instances, this interaction is weak enough to engender high lability of the counterion and high reactivity associated with the electrophilic center. The chelating nature of the borate interaction in complexes **2** appears to render this B–H interaction relatively non-labile as both **2a** and **2b** serve as poor ethylene polymerization catalysts (*vide infra*).

Reaction of the tuck-in methyl zirconocene **1c** with 1 equiv of  $\text{HB}(\text{C}_6\text{F}_5)_2$  was not as clean as the above described chemistry. This reaction appears to be complicated by a lack of regioselectivity the borane reagent exhibits when presented with the two Zr–C bonds in **1c**. The minor product ( $\approx 40\%$ ) is analogous to **2a** and **2b**, based on a characteristic pattern for the methylene protons ( $\delta$  3.33, d,  $^2J_{\text{HH}} = 14.1$  Hz;  $\delta$  2.36, dd,  $^3J_{\text{HH}} = 6.5$  Hz). The major product (eq 2) likely arises from



initial reaction with the terminal Zr–CH<sub>3</sub> group rather than the tucked-in methylene group since  $\text{CH}_3\text{B}(\text{C}_6\text{F}_5)_2$ <sup>17</sup> was also observed in the medium at short reaction times; it subsequently was used up in an unknown reaction that formed the major product in the final mixture. We do not know the structure of the major compound, but it appears to contain a  $\text{Zr}(\text{CH}_3)\text{C}_6\text{F}_5$  structural unit<sup>31</sup> based on a characteristic triplet for Zr–CH<sub>3</sub> at  $0.22$  ppm ( $J_{\text{H-F}} = 8.5$  Hz), which we have observed in other complexes in which  $\text{C}_6\text{F}_5$  transfer to zirconium has occurred. A similar lack of regioselectivity, with its corresponding complexity, was found in the reactions of tuck-in methyl complex **1c** with  $\text{B}(\text{C}_6\text{F}_5)_3$ . This chemistry was therefore not pursued further.

**Reaction of  $\text{Cp}^*(\eta^5, \eta^1\text{-C}_5\text{Me}_4\text{CH}_2)\text{ZrCl}$  with  $\text{B}(\text{C}_6\text{F}_5)_3$ .** Given the propensity of the  $\text{HB}(\text{C}_6\text{F}_5)_2$  reagent to yield compounds with strong, potentially deleterious, hydridoborate metal interactions in the zwitterionic products, we performed analogous chemistry using  $\text{B}(\text{C}_6\text{F}_5)_3$ <sup>10a</sup> as an alkyl abstracting agent instead. As in the reactions with  $\text{HB}(\text{C}_6\text{F}_5)_2$ , the tuck-in chloride and phenyl starting materials gave clean products, with selective reaction at the metallated methylene group. Thus, treatment of **1a** with 1 equiv of  $\text{B}(\text{C}_6\text{F}_5)_3$  in hexanes gave a yellow precipitate whose microanalysis suggested a formula for the expected zwitterion, **3a**. As a solid, the compound is quite stable and may be prepared conveniently in multigram quantities by this method. In solution, however, its behavior is complex

(29) Crowther, D. J.; Borkowsky, S. L.; Swenson, D.; Meyer, T. Y.; Jordan, R. F. *Organometallics* **1993**, *12*, 2897.

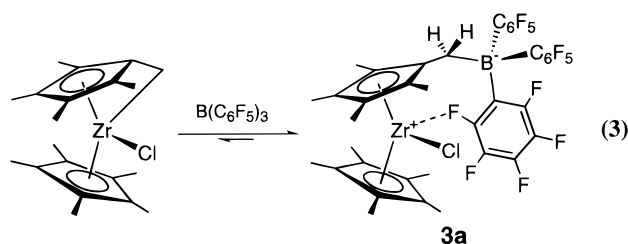
(30) Bazan, G. C.; Schaefer, W. P.; Bercaw, J. E. *Organometallics* **1993**, *12*, 2126.

(31) (a) For example, reaction of  $\text{Cp}_2\text{Zr}(\text{CH}_3)_2$  with  $\text{CH}_3\text{B}(\text{C}_6\text{F}_5)_2$  initially gives a cationic species,  $[\text{Cp}_2\text{ZrCH}_3]^+[(\text{CH}_3)_2\text{B}(\text{C}_6\text{F}_5)_2]^-$ ;  $\text{C}_6\text{F}_5$  transfer to zirconium occurs over the course of about an hour in solution, giving  $\text{Cp}_2\text{Zr}(\text{CH}_3)\text{C}_6\text{F}_5$  and  $(\text{CH}_3)_2\text{BC}_6\text{F}_5$  as the products (ref 31b). Transfer of  $\text{C}_6\text{F}_5$  groups thus appears to be facile from  $\text{R}_2\text{B}(\text{C}_6\text{F}_5)_2$  type counterions, an example of which could arise from initial H/CH<sub>3</sub> exchange in the reaction of **1c** with  $\text{HB}(\text{C}_6\text{F}_5)_2$ . (b) Piers, W. E. Unpublished results.

**Table 3.** Selected Bond Lengths (Å) for **2a**, **3a**, **y-3b**, **o-3b**, and **4**

2a		3a		y-3b		o-3b		4	
Zr(1)–Cl(1)	2.413(3)	Zr(1)–Cl(1)	2.404(3)	Zr–C(76)	2.227(6)	Zr–C(76)	2.195(8)	Zr(1)–H(1)	1.860
Zr(1)–C(14)	2.517(9)	Zr(1)–C(1)	2.589(8)	Zr–C(5)	2.461(5)	Zr–C(5)	2.341(6)	Zr(1)–C(1)	2.546(7)
Zr(1)–C(16)	2.507(10)	Zr(1)–C(2)	2.542(8)	Zr–C(1)	2.511(5)	Zr–C(1)	2.444(6)	Zr(1)–C(5)	2.501(7)
Zr(1)–C(13)	2.477(8)	Zr(1)–C(5)	2.494(8)	Zr–C(4)	2.476(5)	Zr–C(4)	2.487(6)	Zr(1)–C(4)	2.475(7)
Zr(1)–C(15)	2.510(8)	Zr(1)–C(3)	2.505(9)	Zr–C(2)	2.546(5)	Zr–C(2)	2.566(6)	Zr(1)–C(2)	2.463(7)
Zr(1)–C(17)	2.488(9)	Zr(1)–C(4)	2.488(8)	Zr–C(3)	2.560(5)	Zr–C(3)	2.585(6)	Zr(1)–C(3)	2.463(7)
C(18)–B(1)	1.66(1)	C(6)–B(1)	1.67(1)	C(6)–B(1)	1.654(8)	C(6)–B(1)	1.705(9)	C(6)–B(1)	1.66(1)
C(13)–C(14)	1.42(1)	C(1)–C(5)	1.42(1)	C(1)–C(5)	1.433(8)	C(1)–C(2)	1.418(9)	C(3)–C(4)	1.395(9)
C(13)–C(17)	1.42(1)	C(2)–C(3)	1.42(1)	C(2)–C(3)	1.415(8)	C(1)–C(5)	1.431(9)	C(2)–C(3)	1.409(9)
C(14)–C(15)	1.41(1)	C(3)–C(4)	1.42(1)	C(3)–C(4)	1.428(8)	C(2)–C(3)	1.407(9)	C(1)–C(5)	1.418(9)
C(15)–C(16)	1.42(1)	C(4)–C(5)	1.46(1)	C(4)–C(5)	1.445(7)	C(3)–C(4)	1.419(9)	C(1)–C(2)	1.438(9)
C(16)–C(17)	1.43(1)	C(1)–C(2)	1.41(1)	C(1)–C(2)	1.441(8)	C(4)–C(5)	1.428(8)	C(4)–C(5)	1.415(9)
Zr(1)–H(1)	2.01	Zr(1)–F(1)	2.267(5)	Zr–F(65)	2.414(3)			Zr(1)–F(1)	2.237(4)
B(1)–H(1)	1.53	F(1)–C(22)	1.414(9)	C(65)–F(65)	1.415(7)			F(1)–C(22)	1.414(7)
		F(2)–C(23)	1.317(9)	F(64)–F(64)	1.344(7)			F(2)–C(23)	1.320(8)
		Zr(1)–C(6)	3.821	Zr–C(6)	3.330	Zr–C(6)	2.878	Zr(1)–C(6)	3.726
				Zr–C(71)	2.917	Zr–C(71)	2.683		

and spectroscopic evidence suggested the reaction is to some degree reversible.



There are no chelating ion–ion interactions present in **3a** that are strong enough to impose dissymmetric environments on the groups with the same connectivity at room temperature in solution. For example, at room temperature, the proton NMR spectrum of freshly prepared, analytically pure crystals of **3a** exhibited broad featureless peaks, including a peak at 1.74 ppm more typical of a Cp\* ligand in an unreacted tuck-in complex. As the solution samples were cooled, all the peaks broadened until a spectrum compatible with a structure featuring some type of zirconium–borate interaction was observed at 233 K. At this temperature, one major species was present. Its <sup>1</sup>H NMR spectrum consisted of a singlet for the Cp\* ligand (1.34 ppm) and four singlets at 1.28, 1.51, 1.65, and 1.90 ppm for the chemically inequivalent methyl groups of the metallated Cp donor; broad resonances at 3.43 and 2.77 ppm which emerged upon further cooling were attributed to the diastereotopic CH<sub>2</sub>B protons. Other minor compounds were also present, and further spectral changes which we do not fully understand occurred as the sample was cooled to 193 K.

Variable-temperature <sup>19</sup>F NMR spectra were also complicated. At room temperature, sharp signals for a small amount (≈5%) of free B(C<sub>6</sub>F<sub>5</sub>)<sub>3</sub><sup>32</sup> punctuated three very broad peaks in the *ortho*, *meta*, and *para* regions of the spectrum. Lowering the temperatures resulted in the transformation of the broad signals into a complex pattern of multiplets; the spectrum obtained at –61 °C is shown in Figure 2. Six separate resonances for the *meta* fluorines were observed along with three for the *para* fluorine atoms in the region of the spectrum where these groups are normally found. One of the resonances due to the *ortho* fluorines appears far upfield from the others at –167.7 ppm and is consistent with the presence of a species in which one fluorine comes into close contact with the zirconium center.<sup>17,21</sup>

(32) <sup>19</sup>F resonances for *very carefully dried* B(C<sub>6</sub>F<sub>5</sub>)<sub>3</sub> appear at –128.78 ppm (*ortho*), –141.86 ppm (*para*), and –160.14 ppm (*meta*). Minute amounts of water and/or donor solvents such as THF tend to broaden and shift these resonances significantly, particularly that of the *para* fluorines.

Solid-state structural analysis of **3a** indeed revealed a stabilizing dative interaction between an *ortho* fluorine group and the zirconium center (Figure 3). Fluorine(1) occupies a coordination site in the metallocene wedge (Cl(1)–Zr(1)–F(1) = 95.0(1)°), with a Zr(1)–F(1) distance of 2.267(5) Å. This value is shorter than the Zr–F separations of between 2.322(2) and 2.534(3) Å in other zirconocene cations stabilized via lone pair donation from a fluorine<sup>17,21</sup> but still substantially longer than the 1.98(1) Å distance found in Cp<sub>2</sub>ZrF<sub>2</sub>.<sup>33</sup> In addition, the F(1)–C(22) distance of 1.414(9) Å is significantly elongated in comparison to the other C–F bonds in the molecule; the F(2)–C(23) length of 1.317(9) Å included in Table 3 is representative of these bonds.

Alkyl or aryl fluoride coordination to metals outside of the context of group 4 metallocene cations is quite rare,<sup>34</sup> and generally occurs in entropically favored chelating situations such as that observed here. Even chelating F–M donor bonds are intrinsically weak, and as alluded to above, the Zr–F contact observed in the solid state structure of **3a** is labile in solution. The lability of the aryl fluoride ligand in **3b** can possibly be attributed to the strain associated with the chelating arrangement in this complex. In order for fluorine coordination to zirconium to occur in **3a**, the carbon bonded to boron (labeled C(6) in the ORTEP) must tilt out of the plane defined by the Cp carbons away from the zirconium center by 21°. This contrasts with the negligible tilt angle found in **2a**, which did not have to deform in order for the hydridoborate to stabilize the zirconium center via chelation. In comparison, *ortho*-fluorine coordination in a zwitterionic complex reported recently by Erker *et al.*<sup>21a</sup> featuring a –B(C<sub>6</sub>F<sub>5</sub>)<sub>3</sub> group bonded directly to a Cp carbon atom (rather than with an intervening CH<sub>2</sub> group as in **3a**) appears qualitatively to be less prone to dissociation than the present example. In Erker's compound, fluorine coordination is maintained in solution even at room temperature, possibly because the size of the chelate is more suited to the alignment of the C–F dipole moment toward the electropositive zirconium center (C–F–Zr = 150.6(2)°) than in the chelate in **3a**, which is larger by one carbon (C(22)–F(1)–Zr(1) = 124.6(5)°). It therefore appears that in the class of zwitterionic catalysts with borate counterions affixed to a Cp donor, the chelate ring size can have dramatic effects on the strength of the Zr–F interaction and thus the extent to which this particular mode of cation stabilization occurs.

**Reaction of Cp\*(η<sup>5</sup>,η<sup>1</sup>-C<sub>5</sub>Me<sub>4</sub>CH<sub>2</sub>)ZrC<sub>6</sub>H<sub>5</sub> with B(C<sub>6</sub>F<sub>5</sub>)<sub>3</sub>.** The outcome of this reaction was found to be chemically more complex than that discussed above, but the results are illustrative

(33) Bush, M. A.; Sim, G. A. *J. Chem. Soc. A* **1971**, 2225.

(34) Kulawiec, R. J.; Crabtree, R. H. *Coord. Chem. Rev.* **1990**, 99, 89.



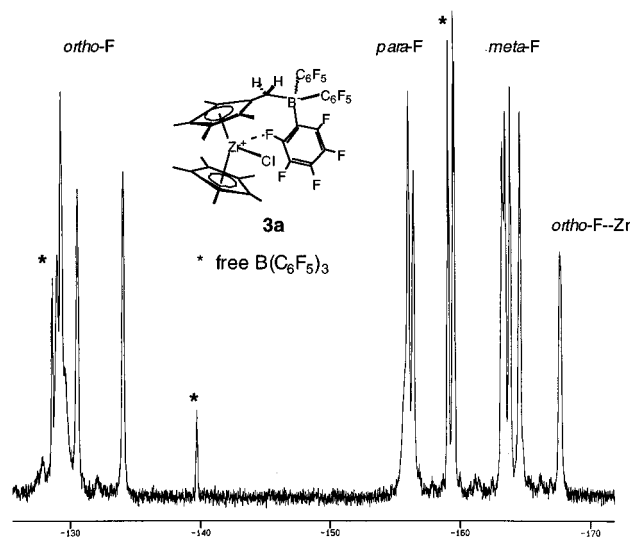


Figure 2.  $^{19}\text{F}$  NMR spectrum of zwitterionic chloride **3a** at  $-61\text{ }^\circ\text{C}$ .

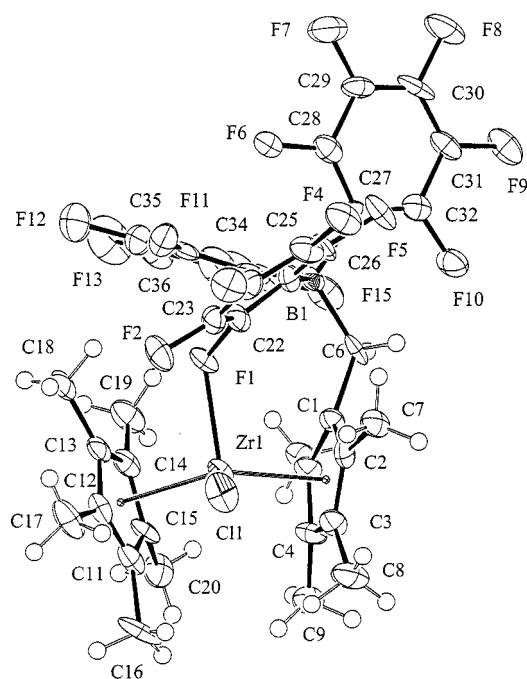


Figure 3. ORTEP drawing of **3a**.

of the subtleties of intramolecular ion–ion interactions in these zwitterionic systems. As in the reaction of tuck-in chloride with  $\text{B}(\text{C}_6\text{F}_5)_3$ , admixing **1b** and the borane in hexanes led to a yellow precipitate that was virtually insoluble in this solvent. If this powder was allowed to remain in the mother liquor and heated gently, large, dark-orange crystals began to form polka dots in the mass of yellow precipitate on the bottom of the flask. Eventually, most of the yellow solid converted to the orange product, **o-3b**, a visually stunning transformation. Alternatively, the yellow product (**y-3b**) could be isolated immediately. Dissolution of this material in  $\text{C}_6\text{D}_6$  resulted in an immediate color change to that characteristic of the orange product. The  $^1\text{H}$  NMR spectra of these particular samples revealed the presence of free hexane in addition to the signals for the orange zwitterion product. Thus, it was not possible to assess the structural differences, if any, between the yellow and orange forms of **3b** by NMR spectroscopy.

Fortunately, X-ray quality crystals of both the kinetic **y-3b** and the thermodynamic product **o-3b** were obtainable. Those for the kinetic product were grown by slow diffusion of a layered hexane solution of tuck-in phenyl complex **1b** into a settled hexane suspension of  $\text{B}(\text{C}_6\text{F}_5)_3$  at room temperature while

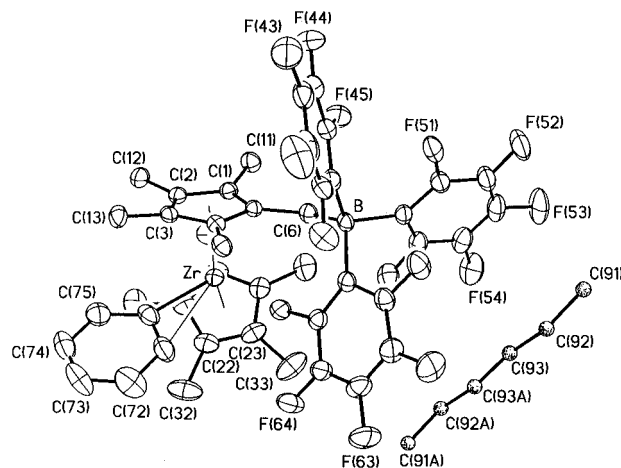


Figure 4. ORTEP drawing of **y-3b**.

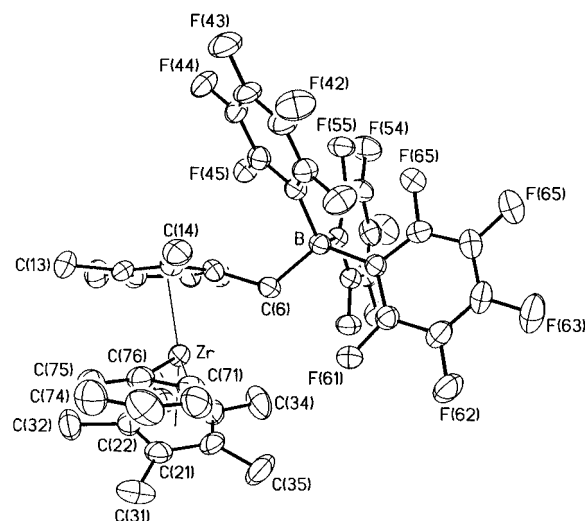
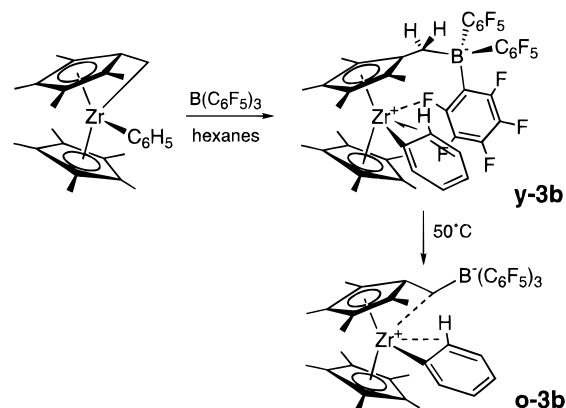


Figure 5. ORTEP drawing of **o-3b**.

#### Scheme 2. Reaction of Tuck-In Phenyl **1b** with $\text{B}(\text{C}_6\text{F}_5)_3$



crystals of **o-3b** were cultivated by more conventional recrystallization techniques. The molecular structures of **y-3b** and **o-3b** are shown in Figures 4 and 5, respectively, and comparable metrical data are given in Tables 3 and 4. Scheme 2 summarizes the chemistry involved based on these structure determinations.

As the NMR experiments suggested, the structure of **y-3b** contains a molecule of hexane in the lattice, but in many ways is similar to that of **3a** in that the zirconium center is again stabilized by dative coordination from an *ortho*-fluorine atom. The  $\text{Zr}-\text{F}(65)$  of  $2.414(3)\text{ \AA}$  distance in **y-3b** is  $\approx 0.15\text{ \AA}$  longer than that in **3a**, allowing the dipole of the  $\text{C}-\text{F}$  bond to align itself toward the positive charge on zirconium more effectively ( $\text{Zr}-\text{F}(65)-\text{C}(65) = 165.2(3)^\circ$ ). The  $\text{Zr}-\text{F}$  attraction is attenuated in **y-3b** because the metal is also receiving electron

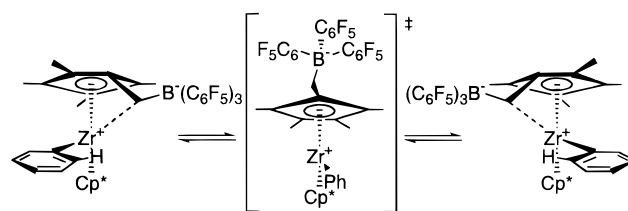
density from an agostic C–H interaction as suggested by the distortions evident in the phenyl group; the steric bulk of the phenyl group relative to a chloride ligand is also a factor. The phenyl group lies in the plane bisecting the Cp donors and the *ipso* carbon is  $\sigma$  bound in one of the *exo* positions of the metallocene girdle. The agostic phenyl interaction is implicated by the much smaller Zr–C(76)–C(71) angle of  $106.0(5)^\circ$  in comparison to the Zr–C(76)–C(75) angle of  $138.0(6)^\circ$ , bringing C(71)–H into much closer proximity to the zirconium center (Zr–C(71) = 2.92 Å) than C(75). A final feature of this structure worth noting is the limited extent to which C(6) is perturbed from the plane of the five Cp carbons. Unlike **3a**, (*vide supra*) the metallated carbon in **y-3b** is tilted slightly toward the metal by about  $6^\circ$ .

The structure of **o-3b** is strikingly different from that of the kinetic product discussed above. As in **y-3b**, the zirconium center is satiated by an *ortho* C–H agostic interaction, but as manifested by the structural parameters, the interaction is stronger in **o-3b**. The phenyl group is canted more severely toward the *endo* coordination site (Zr–C(76)–C(71) =  $94.5(5)^\circ$ ; Zr–C(76)–C(75) =  $149.3(6)^\circ$ ) than in **y-3b**, and the contact distance of 2.683 Å between Zr and C(71) is significantly shorter and more comparable to similar data observed in other  $\beta$ -agostic zirconocene complexes.<sup>19,35</sup> Evidence that the agostic interaction is maintained in solution is sketchy. The agostic structure could not be frozen out at low temperature; signals for the *ortho* and *meta* protons of the phenyl group remained averaged at all temperatures examined. Further, the averaged C–H<sub>*ortho*</sub> coupling constant of  $155 \pm 1$  Hz, while lower than the C–H<sub>*meta*</sub> ( $165 \pm 1$  Hz) and the C–H<sub>*para*</sub> ( $171 \pm 1$  Hz) J values, is not diagnostic.<sup>36</sup>

The biggest difference between **3a** or **y-3b** and the orange polymorph of **3b** is the absence of a close Zr–F contact in the latter compound. Rather, a second stabilizing feature present in **o-3b** involves donation from C(6) to the electron-deficient zirconium center. This interaction is related to the bridging methyl interactions observed in cation-like metallocenes isolated upon treatment of Cp<sub>2</sub>Zr(CH<sub>3</sub>)<sub>2</sub> complexes with B(C<sub>6</sub>F<sub>5</sub>)<sub>3</sub>. Borate ions of the form RCH<sub>2</sub>B<sup>–</sup>(C<sub>6</sub>F<sub>5</sub>)<sub>3</sub>, because of the differences in electronegativity between B and C, exhibit some charge localization on the carbon bonded to boron. The carbon atom thus is capable of donating electron density to vacant orbitals on zirconium when counterions of this type are present.<sup>16,37</sup>

Several lines of structural evidence indicate that the abstracted metallated carbon is engaged in a stabilizing interaction with the metal center in **o-3b**. Unlike the compounds discussed above, the metallated carbon in **3b** is tilted severely out of the plane defined by the Cp carbons toward the zirconium atom by  $24^\circ$ , bringing C(6) to within 2.878 Å of zirconium (compared to a distance of 3.33 Å for the same parameter in **y-3b**). Indeed, bonding of the entire borate-substituted Cp ring is severely distorted from normal, symmetric  $\eta^5$  bonding. The Zr–C(5) distance is only 2.341(6) Å, compared with an average Zr–C separation of 2.519 Å in the unsubstituted Cp\* ligand. The Zr–C(1) and Zr–C(5) bonds are slightly longer at 2.444(6) and 2.487(6) Å, respectively, while bonds to C(2) and C(3) are longer still (Table 3). The tilted bonding mode of this Cp ligand is a consequence of the attraction between the zirconium center and C(6). This interaction is also supported by the alignment of the C(6)–B vector with zirconium (Zr–C(6)–B =  $170.7^\circ$ ),

**Scheme 3.** Fluxional Process Exchanging Diastereotopic Groups in **o-3b**



pointing directly at the remaining *exo* coordination site on the zirconium (compared to an angle of  $35.8^\circ$  for the same parameter in **y-3b**). A further consequence of this interaction is the elongation of the B–C(6) bond (to 1.707(9) Å) in comparison with the same bond in compounds **2a**, **3a**, and **y-3b**. The alignment Zr–C(6)–B also argues against significant agostic C–H character to this interaction which, if present, should give lower values for this angle. The close to normal CH coupling constant of  $121 \pm 1$  Hz (averaged) observed for the methylene CH bonds in **o-3b** supports minimal direct C–H bond involvement in the Zr–C(6) contact.

In comparison to the non-chelating Zr–C<sub>bridging</sub> separations of 2.549–2.640 Å observed for compounds of general formula Cp'<sub>2</sub>Zr<sup>+</sup>Me<sup>–</sup>MeB<sup>–</sup>(C<sub>6</sub>F<sub>5</sub>)<sub>3</sub>,<sup>17,18a</sup> the Zr–C(6) distance is quite long, suggesting that constraining the counterion through covalent attachment to the Cp\* ring attenuates this type of ion–ion interaction. Indeed, in benzene or toluene solution, <sup>1</sup>H NMR spectra of **o-3b** are consistent with an averaged structure at all temperatures examined, *i.e.*, all Cp and phenyl protons with the same connectivity were exchanging on the NMR time scale even at  $-80^\circ\text{C}$ . At this temperature, the signals were severely broadened but had not undergone complete coalescence. The proposed process by which these groups are exchanged is depicted in Scheme 3. Dissociation of the Zr–CH<sub>2</sub>B<sup>–</sup>(C<sub>6</sub>F<sub>5</sub>)<sub>3</sub> interaction leads to a symmetric structure, averaging the environments of related protons. The variable-temperature <sup>19</sup>F NMR spectra are entirely consistent with this hypothesis. At room temperature, the three C<sub>6</sub>F<sub>5</sub> groups are equivalent; at  $-80^\circ\text{C}$  the spectrum shows signals for three separate pentafluorophenyl groups (Table 2).

The process in Scheme 3 is essentially analogous to the ion-pair dissociation mechanism put forward by Marks *et al.* to partially account for exchange phenomena observed in the <sup>1</sup>H NMR spectra of non-zwitterionic complex Cp'<sub>2</sub>Zr<sup>+</sup>Me<sup>–</sup>MeB<sup>–</sup>(C<sub>6</sub>F<sub>5</sub>)<sub>3</sub> (Cp' = 1,2-Me<sub>2</sub>C<sub>5</sub>H<sub>3</sub>).<sup>7b,17</sup> The barrier for ion–pair dissociation at  $80^\circ\text{C}$  in this non-zwitterionic compound is on the order of 18 kcal mol<sup>–1</sup>; since  $\Delta S^\ddagger$  for this process is positive, this barrier rises as temperature decreases. While we were unable to calculate a barrier to the analogous process in the zwitterionic complex **o-3b** with the available data, clearly it is substantially lower than that found for ion–pair dissociation in non-zwitterionic compounds, showing that the strategy of sequestering the counteranion through the design of zwitterionic catalysts can lead to weaker ion–ion interactions.

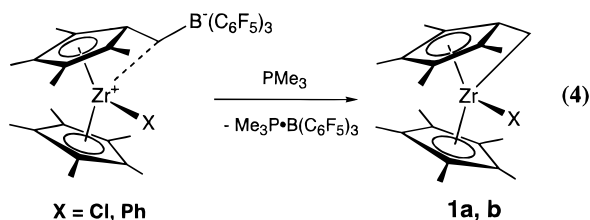
Note that the other process by which methyl groups were exchanged in the non-zwitterionic systems, namely B–CH<sub>3</sub>/Zr–CH<sub>3</sub> exchange based on B–CH<sub>3</sub> bond cleavage, cannot exchange the methylene protons in the zwitterionic compounds discussed here. Nonetheless this process also appears to occur in zwitterions **3** as evidenced by the regeneration of the tuck-in starting materials **1**, with concomitant formation of the adduct Me<sub>3</sub>P·B(C<sub>6</sub>F<sub>5</sub>)<sub>3</sub>,<sup>38</sup> upon treatment of compounds **3a** and **o-3b** with PMe<sub>3</sub> (eq 4). This result is consistent with the observations concerning the solution behavior of **3a** (*vide supra*), which likely proceeds via loss of B(C<sub>6</sub>F<sub>5</sub>)<sub>3</sub> from a structural variant of **3a** akin to that observed in **o-3b**. No evidence for free B(C<sub>6</sub>F<sub>5</sub>)<sub>3</sub><sup>32</sup>

(35) Jordan, R. F.; Bradley, P. K.; Baenziger, N. C.; LaPointe, R. E. *J. Am. Chem. Soc.* **1990**, *112*, 1289.

(36) Brookhart, M.; Green, M. L. H.; Wong, L.-L. *Prog. Inorg. Chem.* **1988**, *36*, 1.

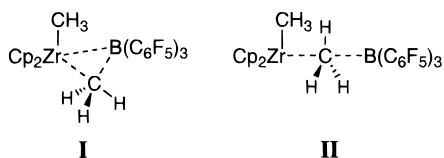
(37) Radius, U.; Silverio, S. J.; Hoffmann, R.; Gleiter, R. *Organometallics* **1996**, *15*, 3737.



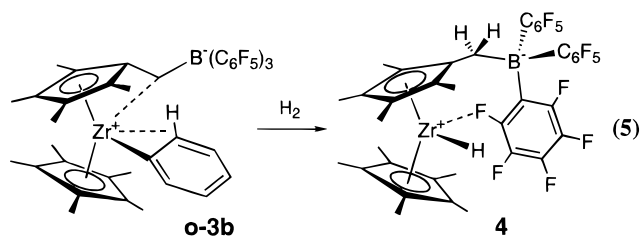


was found for solutions of analytically pure **o-3b** by  $^{19}\text{F}$  spectroscopy, indicating that for this compound the equilibrium is shifted far toward the zwitterion.

The structural attributes of the kinetic **y-3b** and thermodynamic **o-3b** products suggest that the  $\text{B}(\text{C}_6\text{F}_5)_3$  reagent attacks the  $\text{Zr}-\text{C}_{\text{tuck-in}}$  bond from the underside of the metallated carbon (path a, Scheme 4) rather than the top (path b). Although attack from the top would presumably lead directly to the thermodynamically favored polymorph **o-3b**, the borane kinetically prefers the electron density associated with the  $\text{Zr}-\text{C}_{\text{tuck-in}}$  bond, giving **y-3b**. These observations may have some bearing on the mode of abstraction of methyl groups from zirconium by  $\text{B}(\text{C}_6\text{F}_5)_3$  in non-zwitterionic catalysts. Paths a and b in Scheme 4 correspond to two extremes originally proposed by Marks *et al.*<sup>17</sup> for attack of  $\text{B}(\text{C}_6\text{F}_5)_3$  on  $\text{Cp}_2\text{Zr}(\text{CH}_3)_2$ , namely, attack of a  $\text{Zr}-\text{C}$   $\sigma$  bond (I) or the sterically less hindered direct attack on the methyl carbon (II), respectively.



Phenyl zwitterion **o-3b** is stable for several weeks in the solid state ( $-35^\circ\text{C}$ , dark), but is generally a highly reactive species. Reactivity patterns are similar to those observed in other organometallic early metal metallocenes, both neutral and cationic. Like many formally 14 electron metallocenes,  $\sigma$ -bond metathesis reactions with aromatic  $\text{C}-\text{H}$  bonds and  $\text{H}-\text{H}$  are facile.<sup>39</sup> In toluene, the material was converted quite rapidly ( $t_{1/2}$  for loss of **o-3b** was about 20 min) to a mixture of tolyl isomers with elimination of benzene. Similarly, reaction with dihydrogen rapidly leads to expulsion of benzene and formation of a hydride derivative, **4** (eq 5). This highly reactive compound



decomposed in benzene solution in about an hour even in the presence of an atmosphere of dihydrogen, but as a solid, it may be stored at low temperature for several days. The compound

(38) This compound is almost totally insoluble in aromatic solvents and was identified by separate synthesis and comparison of the  $^1\text{H}$  NMR spectra ( $\delta \approx 0.43$  ppm in  $\text{C}_6\text{D}_6$ ). Other phosphine adducts of  $\text{B}(\text{C}_6\text{F}_5)_3$  have been studied: Bradley, D. C.; Harding, I. S.; Keefe, A. D.; Motevalli, M.; Zheng, D. H. *J. Chem. Soc., Dalton Trans.* **1996**, 3931.

(39) (a) Jordan, R. F.; Guram, A. S. *Organometallics* **1990**, *9*, 2116. (b) Jordan, R. F.; Bajgur, C. S.; Dasher, W. E.; Rheingold, A. L. *Organometallics* **1987**, *6*, 1041. (c) Jordan, R. F.; LaPointe, R. E.; Bradley, P. K.; Baenziger, N. *Organometallics* **1989**, *8*, 2892. (d) Guo, Z. Y.; Bradley, P. K.; Jordan, R. F. *Organometallics* **1992**, *11*, 2690. (e) Thompson, M. E.; Baxter, S. M.; Bulls, A. R.; Burger, B. J.; Nolan, M. C.; Santarsiero, B. D.; Schaefer, W. P.; Bercaw, J. E. *J. Am. Chem. Soc.* **1987**, *109*, 203. (f) Watson, P. L. *J. Am. Chem. Soc.* **1983**, *105*, 6491.

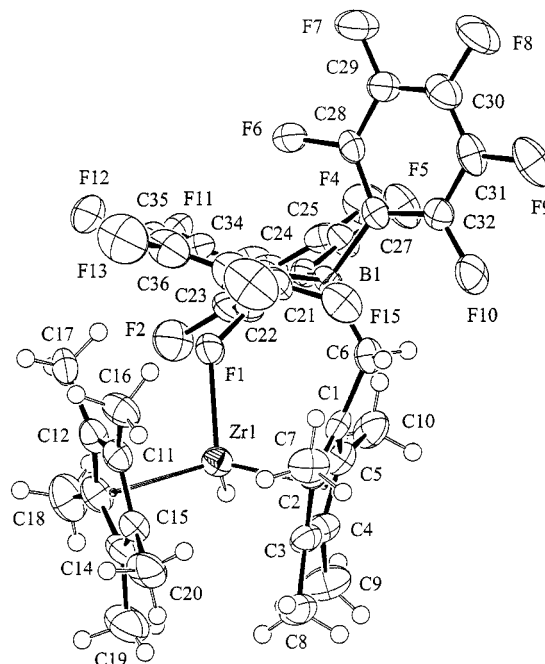
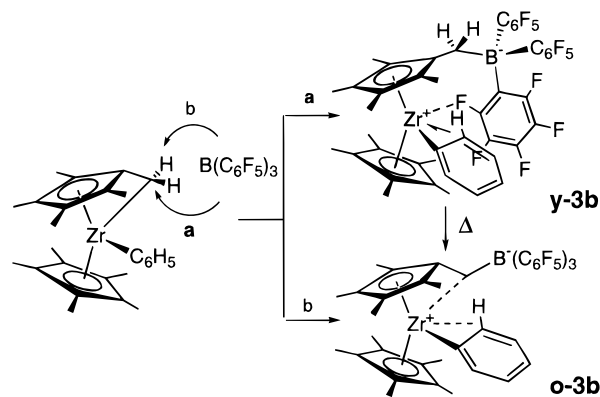


**Figure 6.** ORTEP drawing of **4**.

**Scheme 4.** Trajectories of Borane Attack on Tuck-In Phenyl **1b**



remains a zwitterion as evidenced by the  $^{11}\text{B}$  chemical shift of  $-13.4$  ppm. At room temperature,  $^1\text{H}$  NMR spectra are broadened by an exchange process and are near the coalescence point. Lowering the temperature resulted in the emergence of familiar patterns for a structure with arrested rotation of the metallated ring. From the coalescence behavior of the methylene protons, a rate constant of  $418(2) \text{ s}^{-1}$  (288 K) was calculated for the process that exchanges these groups, corresponding to a barrier of  $13.4 \pm 3 \text{ kcal mol}^{-1}$ . Although the  $^1\text{H}$  NMR spectra are consistent with a process similar to that shown in Scheme 3 above, the  $^{19}\text{F}$  NMR spectra at various temperatures make it clear that hydride **4** is stabilized by a dative  $\text{F} \rightarrow \text{Zr}$  interaction as in **3a** and **y-3b** rather than the  $\text{B}-\text{CH}_2 \cdots \text{Zr}$  Coulombic attraction found in **o-3b**. At  $-55^\circ\text{C}$ , six separate resonances for the *ortho* fluorines were observed in a similar pattern to that described above for the low-temperature  $^{19}\text{F}$  spectra for **3a**, including an upfield shifted signal at  $-147.1$  ppm.

Yellow crystals of hydride **4** were obtainable via slow reaction of a settled suspension of **o-3b** with  $\text{H}_2$  in hexanes; the molecular structure of this compound is shown in Figure 6. As can be seen, the structure is similar to that of **3a**, with  $\text{Zr}(1)-\text{F}(1)$  a relatively short  $2.237(4) \text{ \AA}$  and  $\text{Zr}(1)-\text{F}(1)-\text{C}(22)$  equal to  $129.3(4)^\circ$ . The  $\text{C}(6)$  tilt angle is again away from the zirconium center to the tune of  $+14^\circ$ . The hydrogen attached to zirconium was found on the difference Fourier map and fixed in its

**Table 5.** Ethylene Polymerization with Zwitterionic Catalysts<sup>a</sup>

catalyst	cat (mg)	co-cat. (5 eq)	PE (mg)	PE			
				10 <sup>6</sup> A <sup>b</sup>	10 <sup>-3</sup> M <sub>n</sub>	10 <sup>-3</sup> M <sub>w</sub>	M <sub>w</sub> /M <sub>n</sub>
<b>2a</b>	15	MAO	22	0.0022	50	180	3.6
<b>3a</b>	15	MAO	138	1.0	95	142	1.5
<b>o-3b</b>	20	MAO	117	0.67	29	118	4.1
<b>o-3b</b>	20	none	217	1.3	20	36	1.8
<b>4</b>	19	none	223	1.3	7.4	23	3.0
<b>non-Zwit<sup>c</sup></b>	15	none	206	1.5	16	40	2.4
<b>Cp*<sub>2</sub>ZrCl<sub>2</sub></b>	9	MAO	10	.0049	14	136	9.4

<sup>a</sup> Conditions: 25 °C, 15 psi ethylene, toluene solution. <sup>b</sup> Activity units: (g pol/MolZr·atm·h). <sup>c</sup> [Cp\*<sub>2</sub>ZrMe][MeB(C<sub>6</sub>F<sub>5</sub>)<sub>3</sub>].

position. The Zr–H distance of 1.86 Å compares to that of 2.00(5) Å found in the only other “base-free” cationic zirconium hydride crystallographically characterized.<sup>17,40</sup> Stable cationic zirconium hydrides are still rare; the reactivity of this compound is under active study.

Clearly, the factors which determine how the electrophilic zirconium centers are compensated electronically in these systems are subtle. Probably the most important determinant is the steric bulk of the substituent on zirconium. When this ligand is smaller, such as a chloride or hydride, an *ortho* fluorine is able to coordinate to the zirconium without undue steric interactions between this ligand and the pentafluorophenyl groups of the counterions. The phenyl ligand, however, is of sufficiently large size to disrupt this mode of bonding, and although accessible, the *ortho*-fluorine structure is unstable with respect to the other stabilizing motif. Isomerization to allow donation of electron density from the <sup>δ</sup>-CH<sub>2</sub>B(C<sub>6</sub>F<sub>5</sub>)<sub>3</sub> to zirconium swings the bulky B(C<sub>6</sub>F<sub>5</sub>)<sub>3</sub> group away from the molecular core, lessening steric interactions. The fact that the phenyl group is capable of partially replenishing the electron density lost through disruption of the fluorine donation is also a factor that tips the thermodynamic balance in favor of **o-3b** in this particular system. Upon treatment with hydrogen, the yellow color characteristic of the *ortho*-fluorine-stabilized structure reappears, and this is again the thermodynamically preferred state of the compound.

#### Ethylene Polymerization with Zwitterionic Catalysts.

Each of the new zwitterionic compounds described above was tested for suitability as an ethylene polymerization catalyst. All polymerizations were performed at room temperature under 15 psi of ethylene in toluene following procedures modelled after those described by Marks *et al.*<sup>41</sup> Polymerization data re collected in Table 5. Hydridoborate chelated complexes **2a** and **2b**<sup>42</sup> were poor catalysts, not surprising given the rather strong ion–ion interaction in these compounds. Activities for the other zwitterionic catalysts, alkylated with small amounts of MAO, rivalled those found for non-zwitterionic Marks-type complexes. For comparison, we carried out some experiments using the [Cp\*<sub>2</sub>ZrMe]<sup>+</sup>[MeB(C<sub>6</sub>F<sub>5</sub>)<sub>3</sub>]<sup>-</sup> system under our conditions. In another control experiment, the lack of significant activity observed for Cp\*<sub>2</sub>ZrCl<sub>2</sub> activated similarly with 5 equiv of MAO<sup>43</sup> illustrates the self-activating, single-component nature of these catalysts. Indeed, **o-3b** appears to perform much better in the absence of MAO. The activities reported in Table 5 represent a lower limit since the reactions were undoubtedly mass

transport limited<sup>44</sup> under the conditions we employed. Unfortunately, the data surrendered by these polymerization experiments do not allow for an assessment of the relative activities of zwitterionic versus non-zwitterionic catalysts, which appear to be more or less equal performers under these conditions. More sophisticated experiments are necessary to address this question.

Polymerizations with fluorine-stabilized **3a**/MAO or **4** underwent rapid color changes upon exposure to ethylene from yellow to the darker orange color associated with the CH<sub>2</sub>B-(C<sub>6</sub>F<sub>5</sub>)<sub>3</sub>-stabilized complex **o-3b**. This observation suggests that during the polymerization, when the alkyl group on zirconium is the bulky polymer chain, this latter mode of compensation for the zirconium center is preferred over fluorine donation and is consistent with the observations made concerning how structures change with different wedge ligands.

The polymer samples produced in these experiments had relatively low molecular weights in comparison to those reported for the cation-like systems,<sup>17</sup> likely a function of the different standards employed in the GPC analyses of the polymers (polystyrene<sup>17</sup> vs polyethylene). Polydispersities found for the polyethylenes are closer to reported values and show that the M<sub>w</sub>/M<sub>n</sub> for the zwitterions are between 1.5 and 2.0. The higher value of 4.1 for the **o-3b**/MAO initiated polymerization is probably a reflection of incomplete alkylation of the phenyl complex and the presence of two different active catalysts. In support of this notion, a comparison of the M<sub>n</sub> and M<sub>w</sub> values for the **3a**/MAO and the **o-3b**/none entries suggests that the polymer sample for the **o-3b**/MAO run is essentially a composite of polymers from the former two catalysts.

#### Conclusions

We have prepared several zwitterionic olefin polymerization catalysts from the electrophilic boranes XB(C<sub>6</sub>F<sub>5</sub>)<sub>2</sub> (X = H and C<sub>6</sub>F<sub>5</sub>) and tuck-in complexes of zirconium. The “base-free” nature of these zwitterions renders them highly active toward polymerization of ethylene, with comparable activities to analogous non-zwitterionic catalysts. To the extent that cationic zirconocenes are never completely base-free in condensed media, the zirconium centers in these compounds are sustained electronically via a variety of intramolecular interactions. The strongest (and most damaging from the point of view of polymerization activity) is the chelating borate-type linkage observed in products **2** derived from HB(C<sub>6</sub>F<sub>5</sub>)<sub>2</sub> and the tuck-in precursors. Three separate types of intramolecular stabilizing interactions were observed in zwitterionic complexes obtained from B(C<sub>6</sub>F<sub>5</sub>)<sub>3</sub>: β-agostic interactions for the phenyl compounds, chelating dative fluorine to zirconium bonds from an *ortho*-fluorine atom of the pendant borate moiety, and donation from the carbon attached to boron in the counterion. These interactions differ in importance depending on the steric properties of the reactive ligand in the metallocene wedge.

#### Experimental Section

**General Procedures.** All operations were performed under a purified argon atmosphere in an Inert Atmosphere glovebox or on high-vacuum lines with standard techniques.<sup>45</sup> Solvents were purified as follows: toluene was distilled from sodium benzophenone ketyl and stored over “titanocene”;<sup>46</sup> tetrahydrofuran (THF) was predried with activated (10<sup>-4</sup> Torr, 200 °C, 3 h) 3 Å molecular sieves, distilled from and stored over sodium benzophenone ketyl; hexanes were distilled from lithium aluminum hydride (Aldrich) and stored over “titanocene”;

(44) Janiak, C.; Versteeg, U.; Lange, K. C. H.; Weimann, R.; Hahn, E. *J. Organomet. Chem.* **1995**, *501*, 219.

(45) Burger, B. J.; Bercaw, J. E. *Experimental Organometallic Chemistry*; Wayda, A. L.; Darensbourg, M. Y., Eds.; ACS Symposium Series 357; American Chemical Society: Washington, DC, 1987.

(46) Marvich, R. H.; Brintzinger, H. H. *J. Am. Chem. Soc.* **1971**, *93*, 2046.

(40) Yang, X.; Stern, C. L.; Marks, T. J. *Angew. Chem., Int. Ed. Engl.* **1992**, *31*, 1375.

(41) Giardello, M. A.; Eisen, M. S.; Stern, C. L.; Marks, T. J. *J. Am. Chem. Soc.* **1995**, *117*, 12114.

(42) Data for **2a**/MAO only are given in Table 5; the **2b**/MAO system had poorer activity and the polymer sample obtained therefrom was not analyzed.

(43) Of course, much higher Al/Zr ratios are required to obtain the true activity data for the Cp\*<sub>2</sub>ZrCl<sub>2</sub> catalyst precursor.

**Table 6.** Summary of Data Collection and Structure Refinement Details for **2a**, **3a**, **y-3b**, **o-3b**, and **4**

	<b>2a</b>	<b>3a</b>	<b>y-3b</b>	<b>o-3b</b>	<b>4</b>
formula	C <sub>32</sub> H <sub>30</sub> BF <sub>10</sub> ClZr	C <sub>38</sub> H <sub>29</sub> BF <sub>15</sub> ClZr	C <sub>47</sub> H <sub>41</sub> BF <sub>15</sub> Zr	C <sub>44</sub> H <sub>34</sub> BF <sub>15</sub> Zr	C <sub>38</sub> H <sub>30</sub> BF <sub>15</sub> Zr
fw	742.06	908.11	992.83	949.74	873.66
cryst syst	monoclinic	monoclinic	triclinic	monoclinic	monoclinic
<i>a</i> , Å	16.680(4)	11.977(7)	11.3399(2)	10.074(1)	11.802(3)
<i>b</i> , Å	10.091(2)	18.835(5)	13.7300(2)	19.313(3)	18.438(2)
<i>c</i> , Å	19.388(3)	16.390(7)	16.6497(2)	21.108(3)	16.524(3)
$\alpha$ , deg			95.604(1)		
$\beta$ , deg	108.32(2)	103.45(4)	102.559(1)	94.758(2)	97.98(2)
$\gamma$ , deg			101.829(1)		
<i>V</i> , Å <sup>3</sup>	3097(1)	3595(2)	2448.95(6)	4092.6(9)	3560(1)
space group	<i>P</i> 2 <sub>1</sub> / <i>n</i>	<i>P</i> 2 <sub>1</sub> / <i>c</i>	<i>P</i> 1	<i>P</i> 2 <sub>1</sub> / <i>c</i>	<i>P</i> 2 <sub>1</sub> / <i>c</i>
<i>Z</i>	4	4	2	4	4
<i>F</i> (000)	1496	1816	1006	1912	1752
<i>d</i> <sub>calc</sub> , mg m <sup>-3</sup>	1.591	1.677	1.346	1.541	1.630
$\mu$ , mm <sup>-1</sup>	0.523	0.487	0.312	0.369	0.416
<i>R</i>	0.046	0.060			0.044
<i>R</i> <sub>w</sub>	0.042	0.065			0.033
<i>R</i> 1			0.0577	0.0646	
w <i>R</i> 2			0.1642	0.1429	
gof	1.72	3.69	1.080	1.193	1.89

dichloromethane was distilled from CaH<sub>2</sub>; benzene-*d*<sub>6</sub> was dried sequentially over activated 3 Å sieves and "titanocene" and stored in the glovebox; and other NMR solvents were dried analogously to the perprotio solvents.

Compounds HB(C<sub>6</sub>F<sub>5</sub>)<sub>2</sub>,<sup>23</sup> Cp\*( $\eta^5$ , $\eta^1$ -C<sub>5</sub>Me<sub>4</sub>CH<sub>2</sub>)ZrCl, and Cp\*( $\eta^5$ , $\eta^1$ -C<sub>5</sub>Me<sub>4</sub>CH<sub>2</sub>)ZrPh were prepared according to published procedures.<sup>25,26</sup> B(C<sub>6</sub>F<sub>5</sub>)<sub>3</sub> was purchased from Boulder Scientific Co., and methylaluminoxane (MAO) was obtained from Akzo Nobel as a 7.1% (wt Al) toluene solution. Ethylene was obtained from Matheson and purified by passage through a Matheson Oxiclear disposable purifier (Model No. DGP-250-R1). Other materials were purchased from Aldrich and used as received.

NMR spectra were recorded on Bruker AM200, 300, or WH400 MHz spectrometers. <sup>13</sup>C NMR assignments were made by using the HMQC pulse sequence,<sup>47</sup> which we have found to be useful for detecting resonances for carbons broadened by quadrupolar nuclei and for determining *J*<sub>CH</sub> values. <sup>19</sup>F NMR spectra were referenced externally to C<sub>6</sub>F<sub>6</sub> at -163.0 ppm relative to CFC<sub>13</sub> at 0.0 ppm.<sup>48</sup> <sup>11</sup>B NMR spectra were referenced externally to BF<sub>3</sub>·Et<sub>2</sub>O at 0.0 ppm. Elemental analyses were performed in house on a Control Equipment Corporation Model 440 Elemental Analyzer. GPC analyses of polyethylene samples were carried out at the Nova Chemicals Technology Center, Calgary, Alberta on a Waters 150C GPC instrument under the following conditions: Columns, Shodex AT 10<sup>3,4,5,6</sup> Å; mobile phase, 1,2,4-trichlorobenzene; temperature, 140 °C; flow rate, 1.0 mL/min; concentration, 0.1% (w/v). Molecular weights were calibrated against the standard PE105K obtained from American Polymer Standards Corporation.

**Synthesis of Cp\*( $\eta^5$ , $\eta^1$ -C<sub>5</sub>Me<sub>4</sub>CH<sub>2</sub>)ZrMe (1c).** Benzene (10 mL) was condensed into an evacuated flask containing Cp\*( $\eta^5$ , $\eta^1$ -C<sub>5</sub>Me<sub>4</sub>CH<sub>2</sub>)ZrCl (**1a**, 572 mg, 1.44 mmol) and solid MeLi (42 mg, 1.44 mmol) at -78 °C. The reaction mixture was warmed to room temperature and stirred for 2 h. The benzene was removed *in vacuo*, and the residue was extracted with hexane (15 mL). The solvent was pumped away, and **1c** was isolated as a red powder by filtration. Yield: 450 mg, 83%. <sup>1</sup>H NMR (C<sub>6</sub>D<sub>6</sub>):  $\delta$  1.83 (s, 15H, C<sub>5</sub>(CH<sub>3</sub>)<sub>5</sub>), 1.86, 1.70, 1.58, 1.42 (s, 12H, C<sub>5</sub>(CH<sub>3</sub>)<sub>4</sub>CH<sub>2</sub>), 2.11, 1.63 (d, *J* = 6.6 Hz, 2H, C<sub>5</sub>(CH<sub>3</sub>)<sub>4</sub>CH<sub>2</sub>), -0.94 (s, 3H, CH<sub>3</sub>).

**Synthesis of Cp\*( $\eta^5$ -C<sub>5</sub>Me<sub>4</sub>CH<sub>2</sub>B(C<sub>6</sub>F<sub>5</sub>)<sub>2</sub>( $\mu$ -H))ZrCl (2a).** Benzene (15 mL) was condensed into an evacuated flask containing tuck-in chloride **1a** (200 mg, 0.505 mmol) and HB(C<sub>6</sub>F<sub>5</sub>)<sub>2</sub> (167 mg, 0.483 mmol) at -78 °C. The reaction was warmed to room temperature and stirred for 40 min. The benzene was removed under vacuum and the vessel charged with hexanes (25 mL). The suspension was cooled to -78 °C and filtered cold to afford yellow crystals of compound **2a** (277 mg, 0.373 mmol) in 74% yield. Anal. Calcd for C<sub>32</sub>H<sub>30</sub>F<sub>10</sub>ClBZr: C, 51.80; H, 4.08. Found: C, 51.55; H, 3.26. IR (KBr, cm<sup>-1</sup>):

2993 (sh), 2950 (sh), 2916 (m), 1748 (br,m), 1643 (m), 1514 (s), 1468 (s), 1382 (m), 1277 (m), 1089 (s), 971 (s).

**Synthesis of Cp\*( $\eta^5$ -C<sub>5</sub>Me<sub>4</sub>CH<sub>2</sub>B(C<sub>6</sub>F<sub>5</sub>)<sub>2</sub>( $\mu$ -H))ZrPh (2b).** Pentane (15 mL) was condensed into an evacuated flask containing tuck-in phenyl **1b** (118 mg, 0.270 mmol) and HB(C<sub>6</sub>F<sub>5</sub>)<sub>2</sub> (93 mg, 0.269 mmol) with liquid nitrogen. The reaction mixture was warmed to room temperature and stirred for 1 h. A voluminous yellow precipitate was formed during this period, isolated by filtration, and washed by back distillation of pentane. Yield of **2b**: 132 mg, 0.168 mmol, 62%. Anal. Calcd for C<sub>38</sub>H<sub>35</sub>F<sub>10</sub>BZr: C, 58.24; H, 4.50. Found: C, 58.35; H, 3.96. IR (KBr, cm<sup>-1</sup>): 2988 (sh), 2955 (sh), 2910 (m), 1767 (sh), 1742 (m), 1641 (m), 1513 (s), 1464 (s), 1380 (m), 1279 (m), 1113 (sh), 1088 (s), 971 (s).

**Reaction of Cp\*( $\eta^5$ , $\eta^1$ -C<sub>5</sub>Me<sub>4</sub>CH<sub>2</sub>)ZrMe (1c) with HB(C<sub>6</sub>F<sub>5</sub>)<sub>2</sub>.** Pentane (10 mL) was condensed into an evacuated flask containing tuck-in methyl complex **1c** (20 mg, 0.053 mmol) and HB(C<sub>6</sub>F<sub>5</sub>)<sub>2</sub> (18 mg, 0.052 mmol) with liquid nitrogen. The reaction mixture was stirred for 1 h at -78 °C, warmed to room temperature, and stirred for another hour. The pentane was removed under reduced pressure, leaving an orange powder that was examined by <sup>1</sup>H NMR spectroscopy. <sup>1</sup>H NMR, **2c** (C<sub>6</sub>D<sub>6</sub>): 3.33 (d, 1H, <sup>2</sup>*J*<sub>H-H</sub> = 14.1 Hz, CHHB); 2.36 (dd, 1H, <sup>3</sup>*J*<sub>H-H</sub> = 6.5 Hz, CHHB); 1.56 (s, 15H, C<sub>5</sub>(CH<sub>3</sub>)<sub>5</sub>); 1.93, 1.92, 1.31, 1.30 (s, 12H, C<sub>5</sub>(CH<sub>3</sub>)<sub>4</sub>); Zr-CH<sub>3</sub> and Zr-H-B resonances not found. Major product: 1.85, 1.64, 1.49, 0.22 (t, *J*<sub>H-F</sub> = 8.5 Hz).

**Synthesis of Cp\*( $\eta^5$ -C<sub>5</sub>Me<sub>4</sub>CH<sub>2</sub>B(C<sub>6</sub>F<sub>5</sub>)<sub>3</sub>)ZrCl (3a).** Hexanes (8 mL) were condensed into an evacuated flask containing **1a** (103 mg, 0.260 mmol) and B(C<sub>6</sub>F<sub>5</sub>)<sub>3</sub> (133 mg, 0.260 mmol) at -78 °C. The reaction mixture was stirred for 20 min at -78 °C, warmed to room temperature, and stirred for another hour. The voluminous yellow precipitate formed was isolated by filtration and washed with hexanes. Yield of compound **3a**: 190 mg, 0.217 mmol, 84% yield. Anal. Calcd for C<sub>38</sub>H<sub>29</sub>F<sub>15</sub>ClBZr: C, 50.26; H, 3.22. Found: C, 50.30; H, 3.11. IR (KBr, cm<sup>-1</sup>): 2981 (sh), 2961 (sh), 2918 (m), 1642 (m), 1515 (s), 1455 (s), 1385 (m), 1272 (m), 1084 (s), 1063 (sh), 982 (s), 942 (m), 930 (m).

**Synthesis of Cp\*( $\eta^5$ -C<sub>5</sub>Me<sub>4</sub>CH<sub>2</sub>B(C<sub>6</sub>F<sub>5</sub>)<sub>3</sub>)ZrPh (o-3b).** Hexanes (15 mL) were condensed into an evacuated flask containing **1b** (299 mg, 0.680 mmol) and B(C<sub>6</sub>F<sub>5</sub>)<sub>3</sub> (350 mg, 0.684 mmol) at -78 °C. The reaction mixture was warmed to room temperature and stirred for 1 h, resulting in a yellow precipitate. The yellow slurry was heated at 60 to 55 °C for hours without stirring during which time the yellow precipitate converted to orange crystals. These crystals were isolated by filtration and washed with cold hexanes. Yield of **o-3b**: 530 mg, 0.558 mmol, 82%. Anal. Calcd for C<sub>44</sub>H<sub>34</sub>F<sub>15</sub>BZr: C, 55.64; H, 3.55. Found: C, 54.53; H, 3.29. IR (KBr, cm<sup>-1</sup>): 2954 (sh), 2906 (w), 2867 (sh), 1642 (w), 1514 (s), 1458 (s), 1272 (w), 1083 (m), 977 (m).

**Reaction of Cp\*( $\eta^5$ , $\eta^1$ -C<sub>5</sub>Me<sub>4</sub>CH<sub>2</sub>)ZrMe (1c) with B(C<sub>6</sub>F<sub>5</sub>)<sub>3</sub>.** Pentane (10 mL) was condensed into an evacuated flask containing **1c** (20 mg, 0.053 mmol) and B(C<sub>6</sub>F<sub>5</sub>)<sub>3</sub> (18 mg, 0.052 mmol) with liquid

(47) Bax, A.; Subramanian, S. *J. Magn. Reson.* **1986**, *67*, 565.(48) *NMR and the Periodic Table*; Harris, R. K., Mann, B., Eds.; Academic Press: New York, 1978; p 98.

nitrogen. The reaction mixture was stirred for 1 h at  $-78\text{ }^{\circ}\text{C}$  and warmed to room temperature with stirring for 1 h, resulting in a light orange clear solution. Pentane was removed *in vacuo*, and powder was obtained. The powder was dissolved in  $\text{C}_6\text{D}_6$  to give a red solution and the  $^1\text{H}$  NMR spectrum was recorded.

**Reaction of  $\text{Cp}^*[\eta^5\text{-C}_5\text{Me}_4\text{CH}_2\text{B}(\text{C}_6\text{F}_5)_3]\text{ZrPh}$  (**o-3b**) with  $\text{PMe}_3$ .** Zwitterion **o-3b** (20 mg, 0.053 mmol) was loaded into a sealable 5-mm NMR tube and suspended in  $\text{C}_6\text{D}_6$  ( $\approx 0.7$  mL). The sample was degassed by 2 freeze–pump–thaw routines and  $\text{PMe}_3$  (1 equiv) was condensed into the sample at  $-78\text{ }^{\circ}\text{C}$ . The tube was flame sealed and upon warming to room temperature a white precipitate was formed; this material was centrifuged to the end of the tube. The  $^1\text{H}$  NMR spectrum was recorded and showed quantitative formation of tuck-in phenyl complex **1b**. The white precipitate, highly insoluble in  $\text{C}_6\text{D}_6$ , was shown to be the adduct  $\text{Me}_3\text{P}\cdot\text{B}(\text{C}_6\text{F}_5)_3$  by preparation of an authentic sample as follows. Hexanes (10 mL) and 1 equiv of  $\text{PMe}_3$  were condensed into an evacuated flask containing  $\text{B}(\text{C}_6\text{F}_5)_3$  (354 mg, 0.692 mmol) at  $-78\text{ }^{\circ}\text{C}$ . The reaction was warmed to room temperature and sonicated for 0.5 h, resulting in a white precipitate that was isolated by filtration.

**Synthesis of  $\text{Cp}^*[\eta^5\text{-C}_5\text{Me}_4\text{CH}_2\text{B}(\text{C}_6\text{F}_5)_3]\text{ZrH}$  (**4**).** Hexanes (10 mL) were condensed into an evacuated flask containing  $\text{Cp}^*[\eta^5\text{-C}_5\text{Me}_4\text{CH}_2\text{B}(\text{C}_6\text{F}_5)_3]\text{ZrPh}$  (113 mg, 0.119 mmol) at  $-78\text{ }^{\circ}\text{C}$ . While being warmed to room temperature, the reaction mixture was stirred under 1 atm pressure of  $\text{H}_2$  for 1 h. The resulting yellow precipitate was isolated by filtration and washed once with a portion of cold hexanes. Yield of **4**: 80 mg, 0.092 mmol, 77%. Anal. Calcd for  $\text{C}_{38}\text{H}_{30}\text{F}_{15}\text{BZr}$ : C, 52.24; H, 3.46. Found: C, 51.59; H, 1.91. IR (KBr,  $\text{cm}^{-1}$ ): 2959 (sh), 2917 (w), 2849 (sh), 1644 (m), 1515 (s), 1459 (s), 1383 (w), 1275 (w), 1085 (s), 977 (s).

**Reaction of  $\text{Cp}^*[\eta^5\text{-C}_5\text{Me}_4\text{CH}_2\text{B}(\text{C}_6\text{F}_5)_3]\text{ZrPh}$  with Toluene- $d_8$ .**  $\text{Cp}^*[\eta^5\text{-C}_5\text{Me}_4\text{CH}_2\text{B}(\text{C}_6\text{F}_5)_3]\text{ZrPh}$  was dissolved in toluene- $d_8$  in a flame-sealed NMR tube. Overnight the color of the solution changed from orange to red. The  $^1\text{H}$  NMR spectrum clearly showed the formation of  $\text{C}_6\text{H}_5\text{D}$ . The Cp resonances of the spectrum could not be interpreted.

**General Procedures for Ethylene Polymerization.** Data collected in Table 5 for ethylene polymerizations are the average of at least two runs. Polymerizations were carried out with use of the following procedures, based on procedures reported by Marks *et al.*<sup>42</sup> **Method A:** In a drybox, a 100 mL reaction flask equipped with a large magnetic stirring bar and a septum-covered stopcock sidearm was charged with metallocene catalyst (10–30 mg) and toluene (100 mL). If required, MAO was injected dropwise *via* a syringe at this point into the toluene solution with stirring. An aliquot of this solution (50 mL) was transferred to another 100 mL reaction flask. The two flasks were attached to a vacuum line, and the solutions were degassed by 2 freeze–pump–thaw routines and equilibrated at the desired temperature under vacuum with use of an external constant temperature bath. Gaseous ethylene was next introduced with rapid stirring, and the pressure was maintained at 15 psi. After a measured time interval, the polymerization was quenched by the addition of acidified methanol (3 mL). Methanol (100 mL) was added and the polymer was collected by filtration, washed with methanol (10 mL), and dried *in vacuo* overnight. **Method B:** For polymerizations with catalysts derived from tuck-in methyl derivative **1c**, the procedures are the same as above except that the solutions of **1c** were saturated with 15 psi of ethylene after the solution was degassed and equilibrated at the desired temperature. Polymerizations were initiated by injecting 1 equiv of  $\text{B}(\text{C}_6\text{F}_5)_3$  into the reaction flask through the septum via syringe. Quenching and workup were carried out as described above. **Method C:** For polymerizations with zwitterion **4** as the catalyst, the procedures were as above, except that **4** was generated *in situ* by treating a solution of **3b** with dry  $\text{H}_2$  for 5 min. The hydrogen was removed by exposing the solution to vacuum for a few seconds three times in a row. Polymerization was initiated by admitting 15 psi of ethylene into the vessel; quenching and workup were carried out as described above.

**X-ray Crystallographic Analysis of **2a**, **3a**, and **4**.** A summary of crystal data and refinement details for all structures is given in Table

6. Crystals of **2a** were grown from hexane solution at  $-78\text{ }^{\circ}\text{C}$ . Crystals of **3a** were obtained by slow diffusion of hexane into a concentrated toluene solution of zwitterion at room temperature. Slow reaction of **o-3b** with  $\text{H}_2$  in hexanes yielded yellow nuggets of hydride **4**. Suitable crystals were placed in glass capillaries, sealed, and mounted onto a Rigaku AFC6S diffractometer. Measurements were made with use of graphite monochromated Mo K $\alpha$  radiation at  $-103$ ,  $-73$ , and  $-103\text{ }^{\circ}\text{C}$  for **2a**, **3a**, and **4**, respectively. The structures were solved by direct methods and refined by full-matrix least-squares calculations. The non-hydrogen atoms were refined anisotropically; hydrogen atoms were included at geometrically idealized positions with C–H = 0.95 Å and were not refined. Exceptions were the H-atom bridging Zr and B in **2a** and the hydride ligand in **4**, which were located from a difference map and included at that position. At convergence, *R* and *wR* were 0.046 and 0.042 for **2a**, 0.060 and 0.065 for **3a**, and 0.044 and 0.033 for **4**. The final difference maps were essentially featureless. All calculations were performed with use of the TEXAN<sup>49</sup> crystallographic software package of Molecular Structure Corporation.

**X-ray Crystallography for **y-3b** and **o-3b**.** General: These structures were solved from data collected on the Siemens SMART system on crystals loaded into sealed glass capillaries. In each case, unit-cell parameters were calculated from reflections obtained from 60 data frames collected at different sections of the Ewald sphere. The structures were solved by direct methods, completed by subsequent Fourier syntheses, and refined with full-matrix least-squares methods. All scattering factors and anomalous dispersion coefficients are contained in the SHELXTL 5.03 program library. **y-3b:** Crystals of the kinetically formed yellow polymorph **y-3b** were obtained by layering a solution of tuck-in phenyl complex **1b** in hexanes on top of a settled hexanes suspension of  $\text{B}(\text{C}_6\text{F}_5)_3$ . Slow diffusion at room temperature resulted in large yellow crystals at the interface. No symmetry higher than triclinic was evident from the diffraction data and unit-cell parameters. The E-statistics strongly suggested the centric option and solution in  $P\bar{1}$  yielded chemically reasonable and computationally stable results. A trial application of semiempirical absorption correction based on redundant data at varying effective azimuthal angles yielded  $T_{\text{max}}/T_{\text{min}}$  at unity and was ignored. A molecule of cocrystallized *n*-hexane solvent, disordered along the molecular polar axis, was located at the inversion center and refined isotropically. All non-hydrogen atoms were refined with anisotropic displacement coefficients, while all hydrogen atoms were treated as idealized contributions. **o-3b:** Crystals of the orange thermodynamic polymorph of **3b** were grown from hexanes by slow cooling of a solution heated to  $50\text{ }^{\circ}\text{C}$  for 30 min. The systematic absences in the diffraction data and the determined unit-cell parameters were uniquely consistent for the space group  $P\bar{1}/n$ . Semiempirical absorption corrections were applied based on redundant data at varying effective azimuthal angles. Non-hydrogen and hydrogen atoms were treated as above.

**Acknowledgment.** This work was generously supported by the NOVA Research & Technology Corporation of Calgary, Alberta, NSERC of Canada's Research Partnerships office (CRD program), and the University of Calgary. W.E.P. thanks the Alfred P. Sloan Foundation for a Research Fellowship (1996–98) and Mr. Leon Neumann and Mr. Sunil Chaudry of the Nova Technical Center for GPC measurements on the polyethylene samples.

**Supporting Information Available:** Full listings of crystallographic data for compounds **2a**, **3a**, **y-3b**, **o-3b**, and **4** (72 pages). See any current masthead page for ordering and Internet access instructions.

JA970140H

(49) Crystal Structure Analysis Package, Molecular Structure Corporation, 1985 and 1992.